ClinicSearch

Clinical Trials and Clinical Research

Delia Teresa Sponza *

Open Access

Review Article

Utilization of Spinel Ferrite Nanoparticles in Health Area Like Diagnosis and Treatment of Tumour Cells, Cancer, Magnetic Resonance Imaging, And Drug Delivery and Release

Rukiye Öztekin, Delia Teresa Sponza*

Dokuz Eylül University, Engineering Faculty, Department of Environmental Engineering, Tınaztepe Campus, 35160 Buca/Izmir, Turkey.

***Corresponding Author:** Delia Teresa Sponza, Dokuz Eylül University, Engineering Faculty, Department of Environmental Engineering, Tınaztepe Campus, 35160 Buca/Izmir, Turkey.

Received Date: November 01, 2023; Accepted Date: November 14, 2023; Published Date: December 01, 2023

Citation: Öztekin R., Delia T. Sponza, (2023), Utilization of Spinel Ferrite Nanoparticles in Health Area Like Diagnosis and Treatment of Tumour Cells, Cancer, Magnetic Resonance Imaging, And Drug Delivery and Release, *Clinical Trials and Clinical Research.* 2(6); **DOI:**10.31579/2834-5126/044

Abstract

This paper focuses on the utilization of spinel ferrite nanoparticles (SFNPs) in health area like diagnosis and treatment of tumour cells, cancer, magnetic resonance imaging, and drug delivery and release with more emphasis on the recently published literature studies. The emergence of nanotechnology has revolutionized treatment strategies in medicine, with rigorous research focusing on designing multi-functional nanoparticles (NPs) that are biocompatible, non-toxic, and target-specific. SFNPs offer various applications in biomedical, water treatment, and industrial electronic devices, which has sparked a lot of attention. Current research explores their potential use in hyperthermia and as drug delivery vehicles for cancer therapy. Significantly, there are considerations in applying iron-oxide-based NPs for enhanced biocompatibility, biodegradability, colloidal stability, lowered toxicity, and more efficient and targeted delivery. This review focuses on the synthesis, characterization, and applications of SFNPs in a variety of fields, particularly SFNPs with doping. SFNPs doped with the elements have remarkable electrical and magnetic properties, allowing them to be used in a wide range of applications such as magnetic fields, microwave absorbers, and biomedicine. Furthermore, the physical properties of SFNPs can be modified by substituting metallic atoms, resulting in improved performance. Finally, in this review goes over the synthesis, doping and applications of different types of metal ferrite (Fe2O4) NPs, as well as views on how to choose the appropriate metal Fe2O4 NPs based on the intended application.

Keywords: cancer; diagnosis; drug delivery and release; magnetic resonance imaging (MRI); spinel ferrite nanoparticles (SFNPS); tumour cells

1. Introduction

Spinel ferrite nanoparticles (SFNPs); With its applications in various fields ranging from industrial to biomedical, it attracts a lot of attention and attracts attention. SFNPs in industry; adsorbent and catalyst [1-8]; electronics manufacturing materials [9-14]; and is widely used in wastewater treatment [15-19]. SFNPs in biomedicine; They are very useful in contrast enhancement in magnetic resonance imaging (MRI) [20-24], biomagnetic separation [25, 26], tumor therapy via hyperthermia, drug delivery and release [27-32]. SFNPs are very important in the preparation of modern sensors and biosensors; They are widely used in both industrial and biomedical fields [33-39]. SFNPs have strong antimicrobial activity against some pathogenic microorganisms [40].

Nanoparticles (NPs), refers to materials containing from a few hundred to 105 atoms and having a particle size of less than 100 nm. As the particle size gets smaller especially when the diameter is ≤ 20 nm, SFNPs lose their paramagnetic property and they become superparamagnetic (SPM) responding to an external magnetic field. Each NPs has SPM behavior due to thermal effects; has a critical particle size. NPs show full SPM behavior blocking temperature (TB) = KV/25kB; where, K is the magnetic anisotropy constant, V is the volume of the NPs, and kB is the Boltzmann constant. TB value; particle type, effective anisotropy constant, particle size, applied magnetic field and depends on the experimental measurement time [41-43]. If T < TB, the magnetization increases with T because thermal energy is applied in magnetic fields; It allows magnetic fields to change their direction and align. If T > TB, thermal energy; causing random distortion in magnetic orientation, resulting in higher It causes a decrease in the impact areas and magnetization values [21, 22, 44] (Figure 1).

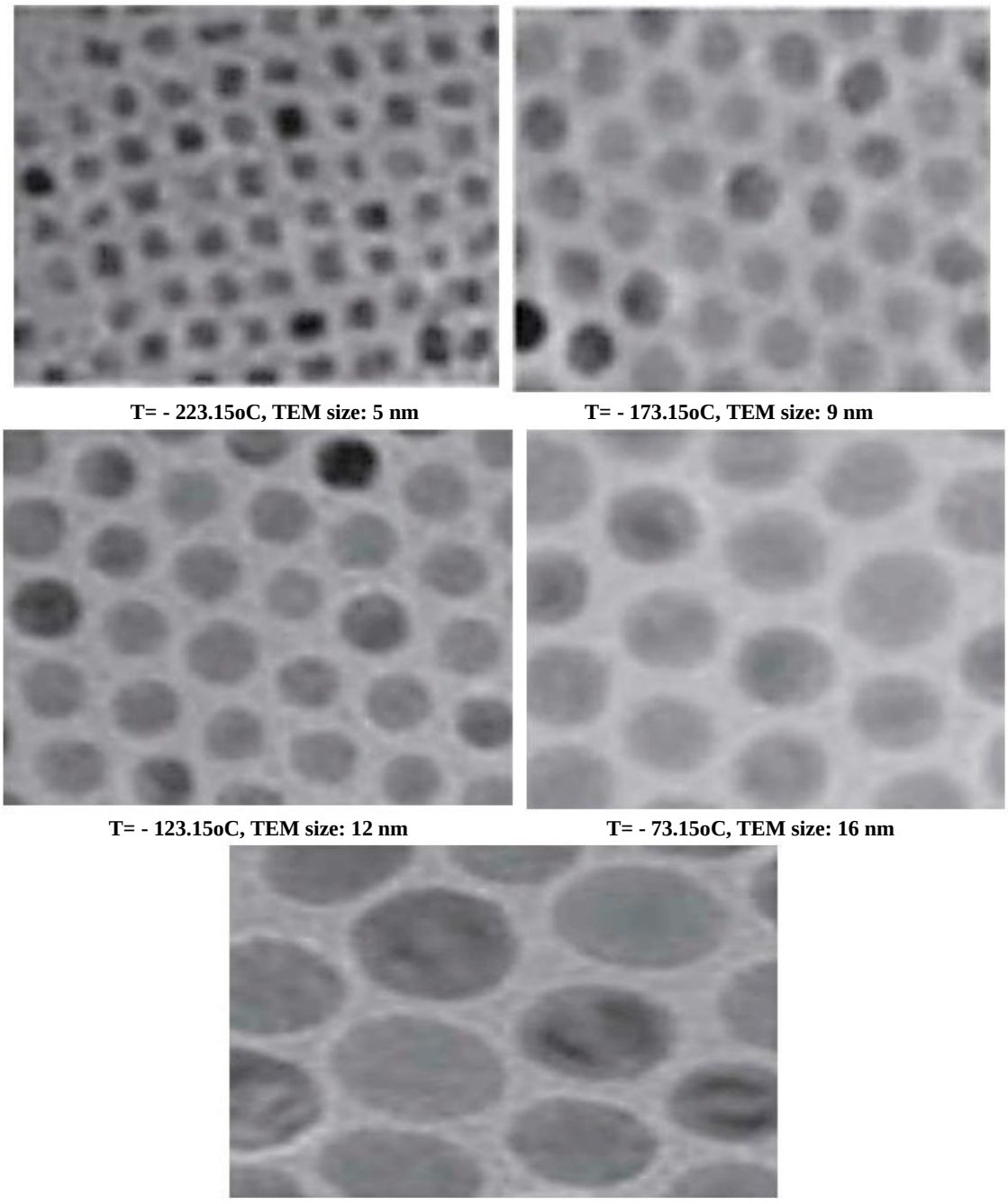

Figure 1: Temperature dependent magnetization TEM images of Fe3O4 SFNPs of different sizes with heat-up method. 5 nm at - 223.15oC, 9 nm at - 173.15oC, 12 nm at - 123.15oC, 16 nm at - 73.15oC and 22 nm at - 23.15oC, respectively (using 100 Oe) [44], Copyright 2004 Nature publishing group.

SPM features allow easy recovery of SFNPs and separated by a low gradient magnetic field [16, 17]. After removing the external magnetic field in the SPM; NPs neither agglomerate nor retain residual magnetism [41, 45-47]. Such inherent properties of SFNPs; It has expanded its use in biomedical applications such as disease diagnosis, MRI, drug delivery, and cancer treatment through hyperthermia. This more important features; It depends on the size, shape, synthesis method, amount and types of additives. The smaller the particle size, the higher the surface area/volume ratio of NPs. For a particle with diameters of 1 μm, 6 nm and 1.6 nm, the atoms in the composition are; about 0.15%, 20%, and 60%, respectively, are on the surface [41, 48]. When these differences in dimensions are compared; unique physical, chemical and mechanical properties also show differences in their collective samples. Among these unique features of SFNPs; SPM and negligible interparticle interactions, these are the key features of SFNPs [49, 50]. By using these unique properties of SFNPs; Many researchers are working to solve current health and environmental problems.

Spinel ferrite-based NPs are metal oxides with spinel structure with the general formula AB2O4. In two different crystallographic regions as tetrahedral (A region) and octahedral (B region); positioned according to the presence of metallic cations containing the least iron. (Figure 2). Net magnetic moment of spinel ferrite; mainly due to the exchange interaction of the valence electrons of the cations in the A and B regions, that is, the cation composition and their distribution over regions A and B, and depends on its magnetic properties. Also, the contribution of A-A and B-B interactions are very low [51, 52]. Distribution of cations; A and B in both regions, the ligand field has a stabilization energy (LFSE).

Synthesis methods may affect the distribution of other cations other than that predicted by the LFSE [53]. Cations in both positions; are tetrahedral and octahedral coordinated to the oxygen atoms. The positions available for 64 tetrahedral and 32 octahedral cations in a unit cell of spinel ferritin; It is occupied by 8 tetrahedral and 16 octahedral cations [51]. Cation types and their distribution in tetrahedral and octahedral regions; It is very important for the physical and chemical properties of SFNPs [53-55]. Depending on the cation distribution types in both regions, three types of spinel structures; known to be normal, reversed and mixed. In normal spinel (such as $ZnFe_2O_4$), cations with oxidation states +2 and +3 occupy tetrahedral and octahedral sites, respectively. In reverse spinel (e.g., Fe_3O_4 and $NiFe_2O_4$); While +3 cations are equally distributed in both regions, all +2 cations are distributed in the octahedral regions. In mixed ferrite [for instance, $MnFe_2O_4$ ($Mn_{0.8}Fe_{0.2}(Mn_{0.2}Fe_{1.8}O_4)$)]; Mixtures of both oxidation states exist in both regions. $CoFe_2O_4$ [chemical formula, $(Co_xFe_{1-x})(Co_{1-x}Fe_{1+x})O_4$]; Depending on the type of synthesis and the conditions used during the synthesis time, it can form an inverted or mixed spinel structure [56].

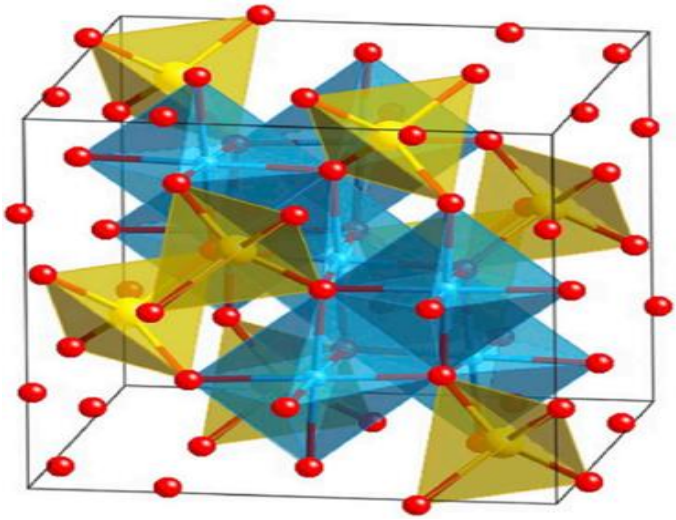

Figure 2: Spinel ferrite structure showing tetrahedral (yellow sites) and octahedral (blue sites regions. Red sites: oxygen atoms. CrystalMaker® was used. http://crystalmaker.com.

Demonstrating the success of SFNPs in cancer therapy and disease diagnosis; There are several current experimental results. Spinel ferrites are approved for use in biomedical applications, with the exception of Fe_3O_4. The main problem in Fe_3O_4; The lack of potential toxicological consequences of short and long-term exposure. To provide maximum benefit from SFNPs in reducing health problems; toxicity due to size, shape, dose, surface chemistry and composition need to be investigated beforehand. SFNPs, as long as safe use information is available; It has endless benefits. Early disease detection, imaging, drug delivery, drug delivery and diagnosis for cancer treatment through hyperthermia; It demonstrated the outstanding and surprising performance of advanced SFNPs.

2. SFNPs Synthesis Methods

Synthesis methods and conditions are the main factors that determine the quality of SFNPs. There is a wide variety of synthesis techniques for SFNPs; co-precipitation [57-61], thermal decomposition [62-65], hydrothermal [12-14, 28, 66-69], solvothermal [70-73], sol-gel [74-77], flame spray pyrolysis [78], sonochemical [79-82], vapor deposition [83], pulsed laser ablation [84, 85], microwave assisted [86-88], microemulsion [89-91], Polyol [92-94], electrochemical [95-98], and mechanical milling techniques [12-14, 53, 99]. Sonochemical and microwave irradiation synthesis methods are new techniques and are increasingly used in the construction of a number of syntheses; In the use of SFNPs, with its advantages such as milder reaction conditions, it provides higher yield, improved selectivity and cleaner reaction [100]. Each method has its own advantages and disadvantages; many parameters such as temperature, solvent type, pH, purity reactants and reaction time can affect the quality of synthesized SFNPs. It has been proven that crystallite size is dependent on reaction time, pH, and temperature [58, 101]. Controlling the synthesis methods and size of magnetic NPs is very important. Generally, SFNPs with a particle size > 25 nm; They exhibit ferromagnetic properties and aggregation tendency at 25oC. SFNPs, which are frequently used in biomedical applications; synthesized either by co-precipitation or thermal decomposition. The co-precipitation synthesis method requires careful adjustment of pH, temperature, ionic strength and appropriate mole ratio of divalent metal to trivalent ion (Fe^{3+}) (1/2) in order to prepare super quality SFNPs. The co-precipitation method is one of the simplest and easiest ways to arrive at SFNPs. Environmentally friendly alkaline aqueous solution is widely used for the synthesis of the size and morphology of controlled NPs [18, 19, 102]. When using the co-precipitation synthesis method, the size of SFNPs can be controlled by temperature or mixing. For the most part, post-annealing is important for stabilization of further synthesized NPs. During thermal degradation, the shape and size of the SFNPs; adjusting the temperature, a heating rate can be controlled by varying the concentration of precursors and the number of organic solvents. Highly monodisperse and uniform NPs; morphology and narrowly distributed particle size, simultaneous surface can be obtained by coating with suitable biocompatible materials [103-105]. In the thermal decomposition method for SFNPs; Since SFNPs with high crytallite and narrow size distribution can be synthesized, it is preferred more than co-precipitation synthesis method in biomedical applications. In SFNPs those produced by the co-precipitation method; They have a wide size distribution and can be combined easily [106, 107]. In terms of simplicity of SFNPs co-precipitation for synthesis, the thermal decomposition synthesis method is more commonly used in crystalline SFNPs with uniform size and shape control [31, 108]. $Mn_{0.6}Zn_{0.4}Fe_2O_4$NPs synthesized by thermal decomposition and on the surface coated with biocompatible thermos sensitive copolymer [109], in vitro examination of synthesized spinel ferrite nanocomposites (SFNCs); narrow size distribution, good drug delivery and showed emission capacity.

For scalable synthesis of uniform iron "heat-up" method for oxide NPs suitable for medical applications has been preferred. The basis of the heat-up method; It is based on slow heating of the reaction mixture of precursors, surfactants, high boiling point solvent from room temperature to high temperature. There is no universal method for the synthesis of SFNPs; Each synthesis method has its own advantages and disadvantages.

3. Biomedical Applications of SFNPs

3.1. Cobalt ferrite ($CoFe_2O_4$)

$CoFe_2O_4$ is one of the most studied SFNPs after Fe_3O_4; It is a hard magnetic material with a face-centered cubic inverted or mixed spinel structure. In its bulk form, high coercivity of ≈ 5.40 kOe [9, 56], It shows high curing temperature at 520°C and saturation magnetization (Ms) of 80 emu/g at 25°C [110, 111]. In medical applications such as drug delivery, tumor treatment with hyperthermia, promising in magnetic resonance imaging (MRI) and medical diagnosis [110-112]. Its properties are like other SFNPs; size, synthesis methods, varies with temperature and pollution [113, 114]. In its bulk form, the main feature of permanent magnetization is; characterized by high coercion. It has lower coercivity values in the range of 0.50–2 kOe in its nano-sized form [115]. The simultaneous increase of coercivity from 1.9 to 4.1 kOe and Ms from 69.5 to 71.4 emu/g was measured by mechanical grinding of $CoFe_2O_4$ to 25 nm with grinding balls [116]. Increase in coercion; relates to stresses induced by mechanical milling. Like other SFNPs, doping of metals; It changes the magnetic properties of $CoFe_2O_4$. Zn^{2+} doped $CoFe_2O_4$ NPs ($Zn_{0.5}Co_{0.5}Fe_2O_4$) synthesized by sol-gel method have high anticancer and antimicrobial activities; High Ms value of 86.6 emu/g, low coercivity of 76 G and residual magnetization of 11.5 emu/g are indicated [117]. $CoFe_2O_4$ NPs and $CoFe_2O_4$ NCs; It is widely used in stress sensor and medical practice [118-120]. Compared with other SFNPs, Co SFNPs has the highest spin-orbital coupling and anisotropy constant. These properties make $CoFe_2O_4$ NPs one of the most important NPs in the field of electronics and biomedicine [9, 110, 111, 121]. High anisotropy of $CoFe_2O_4$ NPs and Ms values leading to favorable magnetic behavior; advantage in biomedical applications [122-124]. $CoFe_2O_4$ NPs: MRI, magnetic separation, magnetically guided drug delivery and in the treatment of cancer with hyperthermia; It is one of the most successful inorganics [110, 111, 125-128]. Since the relaxation of magnetic moment of $CoFe_2O_4$ NPs is much slower; It is preferred more than Fe_3O_4 and γ-Fe_2O_3 with similar dimensions, especially in the treatment of hyperthermia [125, 129]. Although, $CoFe_2O_4$ NPs and Fe_3O_4 NPs have similar size and Ms values; The crystal anisotropy of $CoFe_2O_4$ NPs is greater, and it is more suitable for the treatment of hypertemia and cancer [130]. 5% to 15% doping of traces of Zn^{2+} to $CoFe_2O_4$ NPs (relative to Co); It increased the hyperthermic efficiency of $CoFe_2O_4$ NPs, but further increase of Zn^{2+} concentration had the opposite effect [131]. Possible reason for this; The increase in Ms is due to the displacement of Zn^{2+} in the tetrahedral regions, and thus reduces the magnetic moment of the tetrahedral regions, this causes the total magnetic moments to increase [110, 111, 132]. Ce-Nd doped $CoFe_2O_4$ NPs; It has been found to be effective in the treatment of human colon cancer [133]. Treatment of cancer with hyperthermia is highly dependent on the specific loss power, and is proportional to the Ms values. The increase in Ms values makes NPs the best candidates for cancer therapy.

3.2. Magnetite (Fe_3O_4)

Fe_3O_4 is one of the most widely used SFNPs with its reverse spinel structure. The magnetic moment is largely dependent on the size of the particles; Bulk Fe_3O_4 NPs exhibit ferromagnetic and SPM properties at < 20 nm in size at a curie temperature of 585°C [43]. In the reverse structure, A regions are with Fe^{3+} cations, B regions are equal numbers of Fe^{2+} and it is occupied by Fe^{3+} cations [134]. Fe_3O_4 NPs; MRI is crucial in medical applications such as magnetically guided drug delivery and cancer therapy with hyperthermia [135-139]. Properties of Fe_3O_4 NPs; by changing the particle size or it is modified by doping with transition metals such as Mn, Co, Ni [8, 64, 122, 134, 140]. Mn^{2+} and Zn^{2+} doped with Fe_3O_4 NPs; It has similar saturation magnetization with Fe_3O_4 [141, 142]. Mn^{2+} doped Fe_3O_4 NPs the highest, Zn^{2+} doped Fe_3O_4 NPs showed the lowest rate of hyperthermia. The observed increase is the result of higher SPM single state characters of Mn^{2+} doped Fe_3O_4 NPs; It was associated with the Neel-Brownian relaxation process.

3.3. Maghemite (γ-Fe_2O_3)

γ-Fe_2O_3 is one of the most important spinels containing SFNPs; Structure with 50/3% empty space in the octahedral region: γ-Fe_2O_3 = $[Fe^{3+}]\ A[(5/3Fe^{3+}).1/3V]BO_4$, where V: represents a space [49, 143]. Because of its biocompatibility and non-toxicity; It is widely used in biomedical and industrial fields. γ-Fe_2O_3 NPs size < 20 nm and at 25oC; high Ms value indicates SPM characteristics with low coercive field and high resistance [144, 145]. The unique property of generating heat when exposed to an alternating magnetic field was discovered in 1957 [146]. Its application in tumor treatment has attracted the attention of many researchers. γ-Fe_2O_3 NPs, except for tumor treatment with hyperthermia; MRI contrast enhancement, it is used in many biomedical applications, including bio-magnetic separation and magnetic drug delivery [147]. Bare and coated NPs are applied in various forms such as nanowires, nanorods, nanotubes, and NPs embedded in a matrix [148].

3.4. Manganese ferrite ($MnFe_2O_4$)

$MnFe_2O_4$, which is neither reverse nor normal structure; It is one of the most common spinel ferrites. It generally belongs to a soft magnet with the mixed spinel structure of Mn^{2+}; both A and B sites are partially involved. In bulk form, it has a cure temperature of 550 to 620°C and a Ms of 80 emu/g [149]. Compared with Fe_3O_4 NPs for the same particle size; It has low magnetic anisotropy, high Ms and magnetic permeability [150]. Among the spinel ferrites, biomedical, microwave devices, magnetic recording media, computer memory chips, radio frequency coil manufacturing, transformer cores, rod antennas are of great interest in many areas of telecommunications and electronic engineering [129, 151, 152]. In applications in microwave and electronic device fields; High magnetic permeability and electrical resistance are used [153]. It is used for MRI contrast enhancement and drug delivery in biomedical applications. The MRI contrast capability of $MnFe_2O_4$ NPs is far superior to that of similar size $CoFe_2O_4$ NPs and Fe_3O_4 NPs [154, 155]. To increase the efficiency of cancer treatment with hyperthermia; It is also used as a core or shell [156].

3.5. Nickel ferrite ($NiFe_2O_4$)

$NiFe_2O_4$ is a well-known soft magnet in reverse spinel structure; It has a structure in which Fe^{3+} is located equally in the tetrahedral and octahedral regions, and Ni^{2+} is located in the octahedral region. $NiFe_2O_4$ NPs are widely used as core material in various transformers, inductors and biomedical applications [149, 157]. $NiFe_2O_4$ NPs are low cost; High electromagnetic performance, moderate Ms and good chemical stability are crucial in MRI application [149, 158]. In the quantitative cytotoxicity test of chitosan-coated and uncoated $NiFe_2O_4$ NPs at different pH levels; Both chitosan-coated and uncoated $NiFe_2O_4$ NPs have no cytotoxicity [159]. $NiFe_2O_4$ NPs are used in the treatment of hyperthermia and cell-differentiating cancer. Similar to other SFNPs, $NiFe_2O_4$ NPs: to reduce their degradation rate or increase their biocompatibility; should be coated with suitable biological organic molecules [160].

3.6. Zinc ferrite ($ZnFe_2O_4$)

$ZnFe_2O_4$; It is one of the most studied SFNPs with a normal spinel structure of Zn^{2+} and Fe^{3+} in tetrahedral and octahedral sites. In its bulk form, $ZnFe_2O_4$ NPs are paramagnetic and in the octahedral region, $ZnFe_2O_4$ NPs show ferromagnetic properties due to the partial migration of zinc ions [149]. Application similar to other ferrites; Its electrical and magnetic properties mostly depend on the synthesis method and particle size [161, 162]. In the synthesis of $ZnFe_2O_4$ NPs by conventional combustion method and microwave assisted combustion; There were many differences in particle size and Ms values. While the measured particle size for both methods ranged from 372 to 541.7 nm and 23.4 to 48.5 nm; respectively, 63.61 and 255.7 emu/g correspond to average Ms values [163]. With a higher Ms value such as 255.7 emu/g, particle size is reduced; This is very important information showing that it can be used in the treatment of cancer with hyperthermia. But the corresponding 52.28 Oe coercivity and 54.06 emu/g residual magnetization rates should be reduced. Importance of silica-coated 8 nm $ZnFe_2O_4$ NPs in heart disease diagnosis by mouse experiments highlighted [164]. It has been stated that $ZnFe_2O_4$ NPs have an active role in resetting the heartbeat.

4. Factors Affecting of SFNPs

4.1. Particle size and shape

The particle size and shape of SFNPs; governs to the physical stability of SFNPs, its basic properties such as Ms, coerciveness and residual magnetizations [165, 166]. The unique features of SFNPs arise from finite-size and surface effects that dominate the magnetic behaviour of individual NPs [41]. The magnetic properties of NPs observed that the sole dependence of Ms and residual magnetisations on the size [167], while the coercivity and TB of NPs dominantly affected by both size and shape due to the surface anisotropy effects. For a similar size of γ-Fe2O3 the higher TB were observed for spherical than for cubic NPs [44, 168].

For a different type of SFNPs, there is a critical size for the transition from a magnetic multi-domain state towards a magnetic single-domain state at 25oC. Critical sizes for the observation of single-domain SPM behaviour in a variety of common ferromagnetic fine particles for example, Co, Ni, CoFe2O4, Fe2O3, Fe3O4 and FeO are presented [169]. For some SFNPs, such manifestations of SPM properties have been observed at sizes < 25 nm. Even at such low size levels, there is a difference in SPM properties of the same composition but difference in size. For instance, uniformly sized Fe3O4 of 12 nm, 9 nm, 6 and 4 nm exhibited Ms values of 101 emu/g, 80 emu/g, 43 and 25 emu/g, respectively [170]. As the size decreases, the number of surface ions increases and results in higher surface energy. The higher surface energy of each SFNPs hinders the possible spin alignment of atomic dipoles or the coordination between surface ions decreases and results in low Ms values, reduction of coercivity and residual magnetisation [21, 74, 171]. In fact, the differences in size also result in differences in magnetic anisotropy constant, toxicity, exchange stiffness and other properties of SFNPs, and it is one of the determining factors for SFNPs to be used for biomedical application. In order to eliminate any adverse health impact on the biological system, the SFNPs must have a suitable size and SPM properties [29, 172]. SPM NPs are active only in the presence of an external magnetic field; it becomes diamagnetic if the external magnet is removed from the body and easily eliminated. Generally, the degree of crystallinity, shape, size, ease of dispersibility capacity of SFNPs have importance in biomedical applications.

4.2. Coating application

SFNPs attempted to be used for biomedical treatment are coated for several reasons, among which leachability or reduction of degradation, toxicity, adding new properties to SFNPs to avoid agglomeration, thermal stability and increasing dispersibility are the main reasons [126, 129, 169, 173, 174]. Crystalline spinel ferrites, which sintered at appropriate temperatures are well stable > pH=3.0, as it has been confirmed via leaching test [175-177]. CoFe2O4 NPs cytotoxicity evaluated against different human and rat cell lines showed that low concentration of cobalt ions leachability from CoFe2O4 NPs [178, 179]. The amount of leached Co ions was below the toxicity level to various biological cell line models examined during the study; it has been concluded that any toxicity effect could be attributed to the direct effect of the CoFe2O4 NPs [179]. The cytotoxicity of bare and coated 5.6 nm CoFe2O4 NPs by means of micronucleus test observed 4-fold toxicity of the bare than coated [180]. The embryotoxicity of CoFe2O4 NPs through the embryonic Stem Cell Test method also confirmed the higher toxicity of bare CoFe2O4 NPs than coated by silanes [181], the toxicity knowledge of CoFe2O4 NPs also echoed the same [182]. It has been recommended that coating SFNPs with biocompatible organic or inorganic chemicals, particularly, which are intended to be used for medicinal purpose prevents them from being exposed directly to the body. Coating reduce agglomeration of those SFNPs with high values of Mr and Hc, and reduce their side effects [183, 184]. Such as, Fe3O4 coated with sodium oleate (primary layer) and polyethylene glycol-6000 (secondary layer) improved its thermal stability becaus of the interaction between the Fe3O4 NPs and protective layers [173]. Surface modified Co0.1Ga0.9Fe2O4 NPs by tetra ethylene glycol were synthesised via thermal decomposition [184], the synthesised NPs showed improved Ms, SPM characteristics, hydrophilic character relative to GaFe2O4 NPs, indicating that a potential candidate for biomedical applications. The importance of surface modification of SFNPs with different functional groups having hydrophilic properties, such as polyethylene glycol, silica-gel, and dextran in order to improve the properties of SFNPs and enhance their stability [21]. It is preferable to protect SFNPs from degradation or leaching by coating their surface with suitable biocompatible chemicals (organic or inorganic) specially those which are used for in vivo applications. Coating may also help to retain the core SFNPs properties as well as assisting in functioning properly for their intended purpose. If a proper coating materials selection is not done, changes from the original structure and biodegradation of the synthesised SFNPs may occur when exposed to the biological system. In addition to, coating of SFNPs slightly affect the magnetic moment and also the coated NPs are not as effective as their naked counterparts [120, 185, 186]. The coating thickness and hydrophobicity can drastically affect the magnetic properties of SFNPs and decrease the Ms [187, 188]. For instance, coating CoFe2O4 NPs (50 emu/g) by polyacrylonitrile (PAN) decreased its Ms by 10% (45 emu/g) [189]. Coating CoFe2O4 NPs with oleic acid resulted in very high coercivity of 9.47 kOe and decreased its Ms by 10-fold to 7.1 emu/g [190]. The high coercivity of the composite was attributed to the magnetic anisotropy, strain and disorder of the surface spin developed by covalently bonded oleic acid to the surface of CoFe2O4 NPs. The Ms of NiFe2O4 NPs and its corresponding activated carbon-NiFe2O4 NCs revealed similar facts, namely a decrease in Ms from 47.36 to 18.58 emu/g, and an increase in coercivity from 50 to 90 Oe were obtained [191]. When Fe3O4 NPs were coated with citric acid and Au, a significant decrease in the Ms of Au-coated Fe3O4 NCs (30.2 emu/g) compared to citric acid-coated Fe3O4 NCs (67 emu/g) was measured [61]. Such disparity is mainly attributed to the diamagnetic property of Au NPs. In general, the decrease in a magnetic moment due to coating may be explained in terms of spin pinning. As previously stated, the smaller the size of SFNPs the larger the number of atoms available on the outer surface than the inner. The magnetic contribution of these surface atoms will be affected or quenched because of pinning of the surface spins by coated ligands [192]. In contrast, the non-influence of magnetic properties when SFNPs are coated by phosphonates has been observed [193], showed that these ligands reduce the disorientation of the spin of surface atoms. Clearly, the nature of coating materials and thickness of coating are the determining factors in explaining the differences which arise in the change of the properties of SFNPs. Thus, in order to reduce the negative consequence of SFNPs, it is necessary to minimise the size of the surface coating by controlling the concentration of coating materials and coating time. Their potential cytotoxicity also can be reduced by coating with suitable biocompatible hydrophilic polymers. Unless a suitable coating material is used, coating is always at the risk of SFNPs forming large aggregates or interfering with their useful properties [120, 126, 186]. So, in order to maintain the good performance of SFNPs, improving coating technology or using some other biocompatible dopants that may compensate for the reduced Ms due to coating should be devised by the researchers.

4.3. Chemical structure

The magnetic properties of SFNPs are directly proportional to the chemical compositions, distribution of the cations and type of the cations over tetrahedral and octahedral sites. SFNPs with almost the same size can have different Ms values due to the differences in composition or cation distribution over the tetrahedral and octahedral sites. Such as, a study conducted on a family of 8 nm Co-doped Fe3O4 NPs (CoxFe3-xO4), an improvement on the poor hyperthermic efficiency of Fe3O4 was observed when Fe2+ was substituted by Co2+ [64]. As the Co2+ content increased the specific adsorption rate also increased sharply and reached the optimum value when x = 0.6. The same average size of 3 nm NPs of Zn2+ doped CoFe2O4, an increase in Ms from 72.1 emu/g of CoFe2O4, to 89.7 and 99.7 emu/g for Co0.8Zn0.2Fe2O4 and Co0.6Zn0.4Fe2O4, were observed as the result of doping Zn2+, at 25oC, respectively. The possible reason for the increase in Ms is due to substitution of Zn2+ at the tetrahedral sites and thereby decreasing the magnetic moment of tetrahedral sites, which results in an increase in the total magnetic moments [110, 111, 132]. It shows that it is possible to obtain SFNPs

with new properties by changing the composition by doping different metals without changing the size.

5. Medical applications with spinel ferrite nanoparticles

These nanoparticles were attractive to be used for biomedical applications such as diagnosis of disease, MRI, drug delivery and cancer therapy by hyperthermia. These important properties are highly dependent on size, shape, synthesis method and dopant amount and types.

5.1. Antimicrobial applications with SFNPs

Iron plays a significant role in the development of microbial infections, as many organisms use iron sequestration as a defense mechanism. Microorganisms resistant to Fe+2 and Fe+3 also display unexpected resistance to several antibiotics. MFe2O4 NPs have been shown to possess excellent antibacterial properties against various bacteria and fungi. Escherichia coli has been found to develop resistance to excess iron primarily by changing the way it absorbs iron. CoFe2O4 NPs are commonly used for biomedical purposes because of their ability to combat various human infections. Their high surface area-to-volume ratio and nanoscale size make them effective against harmful microorganisms. A nanocomposite called CoFe2O4@SiO2@Ag, when combined with Streptomycin, has demonstrated significant antibacterial properties against both Gram-positive and Gram-negative microorganisms. The inclusion of Ag NPs on CoFe2O4@SiO2 prevents aggregation and enables easy retrieval from the solution after disinfection through an external magnetic field, owing to the presence of a magnetic core in the composite. CoFe2O4 attaches to microorganism membranes, lengthening the lag stage of the bacterial growth phase, widening microorganism production time, and enhancing bacterial cell division. The antibacterial activity of CoFe2O4 NPs is attributed to the generation of superoxide ($O2^-$) and hydrogen peroxide (H2O2) that exhibit antibacterial properties. The migration of these effective oxides over the cell membrane of bacteria leads to the antibacterial activity of the ferrite NPs against unicellular fungi. ZnFe2O4 NPs have been found to possess effective antibacterial activity against different strains of bacteria, including Lactobacillus, Escherichia coli, Bacillus cereus (which are Gram-positive), and Aeromonas hydrophila and Vibrio harveyi (which are Gram-negative). The antibacterial activity of the NPs was observed to be dependent on their small crystallite size and surface area [40, 51, 194-197].

5.2. Biomedical applications with SFNPs

For use in biomedical applications, magnetic NPs need to have high magnetic saturation values and be biocompatible, while also being stable and non-agglomerated when dispersed in water. These NPs can be used within individual cells to facilitate magnetic fluid hyperthermia, drug delivery, and stimulation of metabolic pathways through thermal excitation. MnFe2O4 NPs have attracted significant interest in the field of biomedicine due to their desirable properties, including simple synthesis, controllable size, high magnetization value, SPM nature, ability to be monitored by an external magnetic field, and high biocompatibility. The surface modification of MnFe2O4 NPs by incorporating them into mesoporous SiO2 nanospheres or coating them with mesoporous SiO2 can enhance the stability of the NPs in water, improve their biocompatibility, and prevent their agglomeration and degradation. The physical properties of CoFe2O4, particularly its great stability, have sparked a lot of interest in possible biomedical applications. CoFe2O4 has been utilized for medication administration, imaging, and brain tumor therapy in general. At high concentrations of CoFe2O4 NPs, metal ions are released, and a portion of these ions can enter cells and lead to cytotoxicity. One possible reason for this could be that the inhibition of cell transcription and protein synthesis leads to changes in cellular function. The adverse effects can be eliminated or reduced by applying a biocompatible SiO2 coating. The coating of CoFe2O4 NPs caused a decrease in their adhesion as the SiO2 matrix possessed a negative charge. The NPs exhibited SPM properties with low Ms values, increased compatibility, and became well-suited for medical applications, including drug delivery to cancer cells and the use of a contrast agent for cancer diagnosis in magnetic resonance imaging [198-202].

5.3. Magnetic resonance imaging (MRI) with SFNPs

One of the most effective medical imaging methods for obtaining diagnosis for clinical purposes is MRI. It's a non-invasive technique that relies on the interaction of protons & biological tissues in the presence of a magnetic field. Briefly, 1 H, 11B, 13C, 19F, or 31P can be used as MRI signal sources because of its sensitivity and abundance in biological tissues, the water proton (1 H) is the most commonly used for clinical purposes [203-207]. As the proton nuclear spin is affected by an external magnetic field, longitudinal magnetization can be observed for imaging purposes. Radiofrequency pulses are used to excite the spin. The longitudinal magnetization decreases in this process, while a transverse magnetization is created. The pulse is removed, and the spin emits energy to return to the ground state. Relaxation is the term for this operation, which is recorded by MRI. The relaxation times T1 (longitudinal: spin–lattice relaxation) and T2 (transverse: spin–spin relaxation), which enable protons to return to their original state, can be used to create an MRI image. The complementation of the NP's magnetic field and its magnetic field and the protons from water molecules are required for T1 and T2. Reducing the resting time limits of water by following tissue separation, using different speeds of tissue regeneration and comparison agents [208]. Presence of Co NPs Ms. (1422 emu/cm3) has a much higher at room temperature than iron oxides (395 emu/cm3), which could result in a stronger proton relaxation effect. This improves MRI contrast and allows for the use of smaller magnetic NPs core without sacrificing sensitivity. Water-soluble Co NPs is difficult to make since [209], they are resistant to oxidation. Larger magnetic particles have a higher r1 relativity than shorter size. Field strength and particle size have little impact on r2 relativity, but the relatively high value of r2 makes Co NPs useful as a negative contrast agent. Other metallic NPs (Fe, Fe\\Ni, Fe\\Co and Fe\\Pt), in addition to Co, can be used as MRI contrast agents. At the same particle size, the r2 and r2* relaxivity of Fe is significantly higher than that of iron oxide [144]. The r2/r1 relaxivity ratio of FePt magnetic NPs is 3–14 times greater than that of standard iron-oxide dependent contrast agents [210]. The lack of specificity in MRI contrast agents is still an issue. Their low sensitivity makes successful identification of tiny targets like tumours in the early stages of cancer [146]. MNPs tend to be an outstanding candidate in this regard. Their magnetic properties, as well as the ease with which they can be modified and regulated in terms of scale, shape, and composition, make them an appealing medium for MRI contrast agents [41, 48, 146, 211]. MNPs have proven to be effective contrast agents. The accumulation of MNPs in the target tissue will alter the local physiochemical properties. They looked at the magnetic properties of a series of spinel structures with the general formula MFe2O4, where M can Ferrite. In the range 85–110 emu/g (Fe + M), there is high saturation magnetization, which has a big impact on the T2 relaxation time. MnFe2O4 outperformed as compared to other ferrites in terms of MRI imaging sensitivity, being able to unambiguously detect small size cancers (~ 50 mg) in vivo documented by some researchers used octapod and spherical magnetic NPs for high-performance T2 contrast agents to successfully detect liver cancer in vivo. Both MNPs were able to detect liver cancer in vivo, but the octapod magnetic NPs were clearly better at distinguishing between healthy and diseased tissue [49, 50, 212, 213].

5.4. Drug delivery with SFNPs

Because of their efficacy, simplicity, ease of preparation, and ability to adapt their properties for particular biological applications, the use of SFNPs as a drug delivery agent under the control of an external magnetic field has gotten a lot of attention [214-216]. Since then, the number of publications in this biomedical area has increased dramatically. Many analyses and research papers involving NPs derived from silica, Au, polymers and other materials are currently available in the literature [54, 55, 214-219]. As a result, it's easy to see that magnetism isn't a necessary

feature when designing a drug delivery nano system, since a wide range of nano materials can be used. However, in recent decades, the use of MNPs in drug delivery has gotten a lot of attention [220]. The traditional method of drug delivery from nonspecific cell and tissue distributions with metabolic instability resulting in whole body toxicity and reduced therapeutic efficacy [221]. Another intriguing feature of SFNPs is their ability to encapsulate cytotoxic drugs within the polymer matrix and deliver them to cells [222]. SFNPs can hold drugs and circulate without spilling, and with the help of an external magnetic field, they can easily travel to the target tumour site and assist in delivering successful therapeutic care to cancer cells by by-passing normal cells [223]. The medication will be released and have therapeutic effects until it reaches the site of action [224]. Multifunctional NPs/NCs, which are made up of SFNPs, anti-cancer drugs, semiconductors (for cell imaging), and biocompatible coating agents, are particularly valuable for cancer therapy. It was used in situ assembly to create multifunctional chitosan-based magnetic hybrid NCs with folateconjugated tetrapeptide composite. Chitosan, CdTe quantum dots, SPM Fe3O4, anticancer agent camptothecin, and folate are the key components of synthesised NCs. MnFe2O4@graphene oxide (GO) NCs with SPM properties was recently synthesised using a sono-chemical process, and the NC has a high doxycycline (DOX) loading potential [224]. The higher DOX loading ability has been due to hydrogen bonding and interactions between GO and DOX, according to the author's observations. In addition, under acidic rather than alkaline conditions, DOX sensitivity and release were found to be higher. As a result, the MnFe2O4@GO is a promising candidate for DOX drug delivery to the tumour site and due to the acidic microenvironment of cancer tissue, the drug could be easily released at the tumour site. It has also been documented that lauric acid capped CoFe2O4 NPs could be used as a promising drug delivery agent with pH sensitive release [225]. Furthermore, capping or coating SFNPs with biocompatible materials may help to improve their stability and reduce their toxicity in cells. To be used for magnetically driven drug delivery, SFNPs must have no residual magnetisation after the external magnet field has been removed, which means they must be SPM. This also allows them to preserve colloidal stability and prevent aggregation, allowing them to be used in biomedical applications [226]. Magnetic attraction between the particles is one of the predicted reasons for SFNPs. Targeted drug delivery with SFNPs has a number of benefits, including minimising drug waste, reducing drug administration frequency, reducing side effects, removing side effects on other organs due to site-specific drug delivery, improving treatment efficacy in a limited amount of time, and being safe and efficient due to drug delivery to preferred target organs. Hyperthermia, drug delivery and release at the target organs, where an increase in temperature to 42oC to 46oC has no direct negative impact on the body.

5.5. Hyperthermia with SFNPs

The basic principle of hyperthermia treatment is to generate heat locally by using an external system to pass energy to the tissue, thus increasing the temperature of the local atmosphere. Observation of certain patients with high fevers led to the development of this physical therapy. Surprisingly, the cancer cells were found to be significantly reduced or completely destroyed. Furthermore, other experiments using radiationresistant cancer cells revealed a promising treatment combination capable of increasing the radiotherapy's efficacy [227, 228]. As a result, hyperthermia will damage, destroy, or make cancerous cells more vulnerable to the effects of radiation and anticancer drugs [229]. To induce heat, various techniques such as ultrasound, microwave, radiofrequency, and others are currently available. The key issue with these thermal methodologies is the absence of homogeneous heat distribution and the depth of therapeutic temperatures (45°C). In this regard, a thermal process based on MNPs is an excellent candidate for addressing these issues. As previously mentioned, their scale, magnetism, and ease of tuning surface properties to accumulate MNPs in tumour tissue are significant advantages. Both of these factors may contribute to the development of a cancertreatment thermal therapy. After an external high frequency or pulsed, electromagnetic field was applied to colloidal magnetic submicron particles phagocytized by cancer cells, local heat was generated. As a result, a highly specific intracellular heat would be produced [230-232]. It was investigated how well they could absorb energy from an external magnetic field of varying intensity and frequency and convert it to heat. In addition, the Zn doped-MNPs ((ZnxMn1-x). Fe2O4 and (ZnxFe1- Fe2O4). Since high values of saturation magnetization were observed for x equal to 0.4, it was possible to observe the mostly positive effect of Zn in the spinel structure of the MNPs studied. For (Zn0.4Fe0.6). Fe2O4 and (Zn0.4Mn0.6). Fe2O4, the values were 161 and 175 emu/g, respectively. HeLa cells were used in a vitro trial, and 84.4% of those treated with (Zn0.4Mn0.6). Fe2O4 died after 10 min, compared to just 13.5 percent of those treated with Feridex®. With all of these findings, it's easy to see how hyperthermia for cancer care has progressed rapidly over time. It was developed developed a coreshell structure compound consisting of MnFe2O4 (shell) and CoFe2O4 (core) for in vivo hyperthermia treatment [233]. In comparison to common antidrug cancers like doxorubicin, the antitumor study in mice showed higher efficacy. It was investigated magnetic hyperthermia therapy. According to the findings, hyperthermia was found to have an important in vivo inhibitory effect on tumour development [234]. The findings in this study strongly suggest that MCLs may be a useful tool in the treatment of prostate cancer. Not only do the MCLs appear to destroy cancerous cells by heating them, but they also appear to cause an immune response. The basic principle of hyperthermia treatment is to generate heat locally by using an external system to pass energy to the tissue, thus increasing the temperature of the local atmosphere. Observation of certain patients with high fevers led to the development of this physical therapy. Surprisingly, the cancer cells were found to be significantly reduced or completely destroyed. Furthermore, other experiments using radiationresistant cancer cells revealed a promising treatment combination capable of increasing the radiotherapy's efficacy [227, 228]. As a result, hyperthermia will damage, destroy, or make cancerous cells more vulnerable to the effects of radiation and anticancer drugs [235]. To induce heat, various techniques such as ultrasound, microwave, radiofrequency, and others are currently available. This regard, a thermal process based on MNPs is an excellent candidate for addressing these issues. As previously mentioned, their scale, magnetism, and ease of tuning surface properties to accumulate MNPs in tumour tissue are significant advantages. Both of these factors may contribute to the development of a cancertreatment thermal therapy [236]. It was described that a "modern multidisciplinary "intracellular" biophysical treatment of cancer" in 1979. After an external high frequency or pulsed, electromagnetic field was applied to colloidal magnetic submicron particles phagocytized by cancer cells, local heat was generated [237]. As a result, a highly specific intracellular heat would be produced. It was created an aqueous magnetic fluid with dextran-modified SPM iron oxides in 1993. It was investigated how well they could absorb energy from an external magnetic field of varying intensity and frequency and convert it to heat [238]. The SFNPs of less than 20 nm were releasing heat by Neel relaxation mechanism while Brown relaxation mechanism in case of large NPs size. The frequency and amplitude of the applied external magnetic field would be > 0.5 × 1010 A/ms [212], and NP sizes range from 10 to 100 nm for safe hyperthermia cancer therapy [239]. If bulk particles have multiple domains, it is limited to be used in magnetic hyperthermia treatment due to magnetization reversal taking place by the magnetic moments flipping in domains where it is antiparallel to the AMF. It also occurs by domain growth in other domains, which occurs at lower fields. If the applied magnetic fields can fully saturate the magnetization, then the energy losses in multidomain materials depend on coercivity. Thus, for fully saturated magnetic materials, the power loss should decrease with an increase in the domain size. As a result, to minimize the power loss, multidomain particles should be avoided. It was also highlighted that SF has the potential to be outstanding contrast agents with respect to MRI image quality contrast, sensitivity, and specificity, as well as potential drug-loaded nanocarrier targets. SF exhibits magnetic anisotropy, which is influenced by the anisotropy of the cations, the symmetry of the interstitial sites, as well as the metal type content and cationic arrangement; some toxic cations such as Sr, La, Y,

Mn, Ag, or Al should be avoided. Within the close-packed arrangement of 32 oxygen ions, most SFs contain a cubic unit cell belonging to the Fd3m space group, in which 24 metal ions are arranged in 8 tetrahedral and 16 octahedral positions [240]. The substituted cations such as Ni, Cu, Co, Mn, Mg, and Zn cause O2 displacement due to the substitution of cations at the tetrahedral sites and have to be expanded. On the other hand, the decrease in the lattice constant in SF systems can be explained by several factors: (1) the doping cation has a smaller ionic radius than the excited cation; (2) a potential rearrangement of Fe2+ and Fe3+ ions takes place inside the tetrahedral/octahedral ionic sites, leading to significant changes in magnetic characteristics; (3) Fe3+ is forced to the tetrahedral sites by a proportion of Fe2+ ions occupying the octahedral sites against their structural preferences that affect the optical, electrical, and magnetic properties of SFs [237-247]. In general, the magnetic behavior of SFs is highly dependent on the cation distribution between tetrahedral and octahedral sites [239]. Because the octahedral site and tetrahedral site spins align antiparallel, one can increase the magnetization in SFs by substituting cations for ferrous and ferric ions. For example, the substitution of Zn2+ by Fe2+ cations in the tetrahedral site gives ZnFe2O4, which exhibits magnetic behavior than Fe3O4 along with high magnetic saturation due to Zn2+ and Fe3+ cations occupying tetrahedral and octahedral sites, respectively. In general, smaller positive ions prefer to occupy the lower coordination site, i.e., the tetrahedral site, due to their relative sizes. The larger positive ions tend to occupy higher-coordination sites, such as octahedral sites [242]. As the Zn fraction increases in the tetrahedral site, the magnetization increases. This approach of cation After surface modification of ferrite NPs with mesoporous SiO2 layer, the surface area of the samples increased from 2.59 to 199.2 m2/g. When compared to pure ferrites, the magnetic characteristics of core–shell samples were reduced. The drug IBU was used to test NPs' ability to store and release the medicine. IBU loading was high and the drug release was regulated in the CuFe2O4@SiO2 NCs system. Following the synthesis of a hybrid core–shell structure, the samples' storage capacity increased from 4% to 34%. The NCs's mesoporous structure and increased surface area resulted in these enhancements. The rate of drug release was reduced when the calcination temperature increased but the release mechanism was unaffected. The cytotoxicity of CuFe2O4 NPs was lowered and the drug release characteristics were improved by coating them with mesoporous silica. This coating, however, limited the potential to generate hyperthermia. Although, the capacity to heat the samples was reduced when CuFe2O4@SiO2 NCs was synthesized, it increased biocompatibility and drug storage [241]. The results suggested CuFe2O4@SiO2 NCs be a promising option for medicinal applications as a hybrid system that can release medications and create heat at the same time. It was combined TiO2 NPs with CoFe2O4 NPs via microwave heating, which was subsequently electrospun into CS/CoFe2O4/TiO2 NCs nanofibers. They tested the impact of DOX hydrochloride-loaded electrospun CS/CoFe2O4/TiO2 NCs nanofibers on melanoma cancer B16F10 cell lines to check whether heat and therapy could be combined. CoFe2O4 NPs were made via microwave heating. TiO2 NPs were mixed with CoFe2O4 NPs to control the temperature increase. The DOX loading efficiency and in vitro drug release of DOX from nanofibers were investigated using an AMF and without a magnetic field under physiological and acidic conditions. As seen in SEM images, the surface of nanofibers was smooth, and no drug crystals were visible on the nanofibers' surface. As a consequence, DOX molecules were well incorporated into electrospun fibers. The anticancer effects of the nanofibers generated were also tested on the melanoma cancer B16F10 cell lines. According to the results, DOX-loaded electrospun CS/CoFe2O4/TiO2 NCs nanofibers may be used for localized cancer treatment. According to in vitro cell incubation tests, simultaneous loading of DOX and CoFe2O4/TiO2 NCs into CS nanofibers following the application of a magnetic field enhanced the cytotoxicity of the nanofibers. The generated CoFe2O4 NPs and CoFe2O4/TiO2 NCs had maximum Ms values of 90.5 and 81.2 emu/g, respectively. The reduction in Ms of CoFe2O4/TiO2 NCs may be explained by the addition of TiO2 NPs. The coercivity values (Hc) of NPs composed of CoFe2O4 NPs and CoFe2O4/TiO2 NCs were 830 and 640, respectively. The fact that CoFe2O4 NPs are smaller and more homogeneous than the manufactured CoFe2O4/TiO2 NCs may explain this behavior.

6. Antibacterial Activities of the SFNPs

The antibacterial activities of the transition metal-substituted CoFe2O4 NPs against E. coli and S. Aureus were performed. All tests were repeated ten times aft er culture incubation at 37°C overnight. Th e concentration of CoFe2O4 NPs was fi xed at 1 g/l. Compared to the control (the sample of bacteria solution without adding NPs), CoFe2O4 NPs and transition metal-substituted Co. Fe2O4 NPs inhibit the growth of both E. coli and S. aureus, and the E. coli killing rate of all Fe2O4 NPs is higher than the S. aureus killing rate. The antibacterial properties of manganese (Mn) and Ni-substituted CoFe2O4 NPs are lower than the pure CoFe2O4 NPs. However, their antibacterial abilities became more dominant when copper (Cu) and zinc (Zn) were substituted into CoFe2O4 NPs. There are several possible mechanisms for the antibacterial action of Zn and CoFe2O4 NPs. Studies suggested that when E. coli is treated with Cu NPs, changes take place in its cell membrane morphology [240]. Cu2+ ions cause destruction of the bacterial cell wall, degradation and lysis of the cytoplasm; leading to cell death. Moreover, high concentrations of Cu NPs demonstrate complete cytotoxicity against E. coli [242]. NPs have a large surface area; thus, their bactericidal efficacy is enhanced compared to large sized particles. Hence, NPs are believed to impart cytotoxicity to microorganisms. For the Zn NPs system, studies showed that Zn binds to the membranes of microorganisms, similar to mammalian cells, prolonging the lag phase of the growth cycle and increasing the generation time of the organisms so that it takes each organism more time to complete cell division [241]. Another proposition maintained that the main chemical species contributing to the occurrence of the antibacterial activity were assumed to be active oxides; for example, H2O2 and O2 –, generated from the surface of the Zn ceramics [244]. These active oxides readily penetrate the cell wall of bacteria and cause cell destruction. Th e penetration rate of active oxides through the bacteria cell wall plays an important role in the killing rate of ZnFe2O4 NPs against bacteria. Furthermore, the structure and chemical composition of the cell walls are quite diff erent between E. coli and S. aureus. The E. coli cell wall consists of lipid A, lipopolysaccharide and peptidoglycan; whereas the cell wall of S. aureus consists mainly of peptidoglycan [245]. Th e results indicate that active oxides generated from transition metal-substituted CoFe2O4 NPs have more capability to penetrate the cell wall and decrease the cell division of E. coli rather than S. aureus [243]. However, the precise mechanism of interaction between bacteria (E. coli and S. aureus) and transition metal-substituted CoFe2O4 NPs needs to be investigated further.

7. Conclusions

In this review focuses on the utilization of SFNPs in health area like diagnosis and treatment of tumour cells, cancer, magnetic resonance imaging, and drug delivery and release with more emphasis on the recently published literature studies. SFNPs have received a lot of attention due to its unique features, including stability under mechanical, chemical, and thermal conditions, high coercivity, elevated anisotropy constant and Curie temperature, high electrical resistance, moderate saturation magnetization, and minimal eddy current loss. SFNPs offer various applications in biomedical, water treatment, and industrial electronic devices, which has sparked a lot of attention. It was investigated on the synthesis, characterization, and applications of SFNPs in a variety of fields, particularly SFNPs with doping. SFNPs doped with the elements have remarkable electrical and magnetic properties, allowing them to be used in a wide range of applications such as magnetic fields, microwave absorbers, and biomedicine. Among all the reviewed synthesis strategies, the usefulness of SFNPs in many applications depends largely on the synthesis processes; efficient synthesis processes yield SFNPs that can function better and endure the conditions under which they are synthesized. As a result, the cost-effective synthesis of large amounts of SFNPs with monodisperse size and shape for a biomedical purpose, however, needs more study and it is

important to take into account and thoroughly examine the toxicity of specific SFNPs. Significantly, there are considerations in applying SFNPs for enhanced biocompatibility, biodegradability, colloidal stability, lowered toxicity, and more efficient and targeted delivery. Current research explores their potential use in hyperthermia and as drug delivery vehicles for cancer therapy. The synthesis, doping and applications of different types of metal SFNPs, as well as the views on how to select suitable SFNPs according to the intended application are examined in detail.

SFNPs have emerged as a promising material for the advancement of nanotechnology and nanomedicine. SFNPs have a variety of medical applications, including cancer diagnostics, cancer gene therapy, and drug administration. In biomedical applications, the efficacy of SFNPs is more dependent on Fe2O4. These NCs make them an interesting medium for biomedical applications. In general, the excellent properties of SFNPs observed, as well as the ease with which they can be functionalized by coating their surfaces with non-toxic chemicals, provide an exciting opportunity for future generations to solve environmental and medical problems. SFNPs, in particular, are highly beneficial in the treatment of cancer. Recent conventional methodologies and approaches to SFNPs synthesis are discussed in this study.

Acknowledgement

This research study was undertaken in the Environmental Microbiology Laboratories at Dokuz Eylül University Engineering Faculty Environmental Engineering Department, Izmir, Turkey. The authors would like to thank this body for providing financial support.

References

1. Senapati, K.K., Borgohain, C., Phukan, P. (2011). Synthesis of highly stable CoFe2O4 nanoparticles and their use as magnetically separable catalyst for Knoevenagel reaction in aqueous medium. *J. Mol. Catal. A Chem*; 339: 24–31.
2. Flores, R.G., Andersen, S.L.F., Maia, L.K.K., José, H.J., de Fatima Peralta Muniz Moreira, R. (2021). Recovery of iron oxides from acid mine drainage and their application as adsorbent or catalyst. J. Environ. Manag; 111: 53–60.
3. Faria, M.C.S., Rosemberg, R.S., Bomfeti, C.A., Monteiro, D.S., Barbosa, F., et al. (2014). Arsenic removal from contaminated water by ultrafine d-FeOOH adsorbents. *Chem. Eng. J*; 237:47–54.
4. Wei, J., Zhang, X., Liu, Q., Li, Z., Liu, L., et al. (2014). Magnetic separation of uranium by CoFe2O4 hollow spheres. *Chem. Eng. J*; 241:228–234.
5. Zhao, X., Wang, W., Zhang, Y., Wu, S., Li, F., et al. (2014). Synthesis and characterization of gadolinium doped cobalt ferrite nanoparticles with enhanced adsorption capability for Congo *Red. Chem. Eng. J*; 250:164–174.
6. Mahfouz, M.G., Galhoum, A.A., Gomaa, N.A., Abdel-Rehem, S.S., Atia, A.A., et al. (2015). Uranium extraction using magnetic nano-based particles of diethylenetriamine-functionalized chitosan: equilibrium and kinetic studies. *Chem. Eng. J*; 262:198–209.
7. Tan, L., Liu, Q., Jing, X., Liu, J., Song, D., et al. (2015). Removal of uranium (VI) ions from aqueous solution by magnetic cobalt ferrite/multiwalled carbon nanotubes composites. *Chem. Eng. J*; 273:307–315.
8. Ibrahim, I., Ali, I.O., Salama, T.M., Bahgat, A.A., Mohamed, M.M. (2016). Synthesis of magnetically recyclable spinel ferrite (MFe2O4, M = Zn, Co, Mn) nanocrystals engineered by sol gel-hydrothermal technology: high catalytic performances for nitroarenes reduction. *Appl. Catal. B Environ*; 181:389–402.
9. Mohamed, R.M., Rashad, M.M., Haraz, F.A., Sigmund, W. (2010). Structure and magnetic properties of nanocrystalline cobalt ferrite powders synthesized using organic acid precursor method. *J. Magn. Magn. Mater*; 322:2058–2064.
10. Tang, S.C.N., Lo, I.M.C. (2013). Magnetic nanoparticles: essential factors for sustainable environmental applications. *Water Res*; 47:2613–2632.
11. Hasanzadeh, M., Shadjou, N., de la Guardia, M. (2015). Iron and iron-oxide magnetic nanoparticles as signal-amplification elements in electrochemical biosensing. *TrAC Trends Anal. Chem*; 72:1–9.
12. Zhang, H., Zhang, X., Lin, H., Wang, K., Sun, X., et al. (2015). Graphene and maghemite composites-based supercapacitors delivering high volumetric capacitance and extraordinary cycling stability. *Electro him. Acta*; 156:70–76.
13. Zhang, J., Song, J.-M., Niu, H.-L., Mao, C.-J., Zhang, S.-Y., et al. (2015). ZnFe2O4 nanoparticles: synthesis, characterization, and enhanced gas sensing property for acetone. Sens. *Actuators B Chem*; 221:55–62.
14. Zhang, Z., Yao, G., Zhang, X., Ma, J., Lin, H. (2015). Synthesis and characterization of nickel ferrite nanoparticles via planetary ball milling assisted solid-state reaction. *Ceram. Int*; 41:4523–4530.
15. Brar, S.K., Verma, M., Tyagi, R.D., Surampalli, R.Y. (2010). Engineered nanoparticles in wastewater and wastewater sludge-Evidence and impacts. *Waste Manag*; 30:504–520.
16. Qu, X., Brame, J., Li, Q., Alvarez, P.J.J. (2013). Nanotechnology for a safe and sustainable water supply: enabling integrated water treatment and reuse. *Acc. Chem. Res*; 46:834–843.
17. Qu, X., Alvarez, P.J.J., Li, Q. (2013). Applications of nanotechnology in water and wastewater treatment. *Water Res*; 47:3931–3946.
18. Kefeni, K.K., Mamba, B.B., Msagati, T.A.M. (2017). Application of spinel ferrite nanoparticles in water and wastewater treatment: a review. *Separ. Purif. Technol*; 188:399–422.
19. Kefeni, K.K., Msagati, T.A.M., Mamba, B.B. (2017). Ferrite nanoparticles: synthesis, characterisation and applications in electronic device. *Mater. Sci. Eng. B*; 215:37–55.
20. Zhu, X., Zhou, J., Chen, M., Shi, M., Feng, W., et al. (2012). Core–shell Fe3O4@NaLuF4: Yb,Er/Tm nanostructure for MRI, CT and upconversion luminescence tri-modality imaging. *Biomaterials*; 33:4618–4627.
21. Lee, H., Shin, T.H., Cheon, J., Weissleder, R. (2015). Recent developments in magnetic diagnostic systems. Chem. Rev; 115:10690–10724.
22. Lee, N., Yoo, D., Ling, D., Cho, M.H., Hyeon, T., et al. (2015). Iron oxide-based nanoparticles for multimodal imaging and magnetoresponsive therapy. *Chem. Rev*; 115:10637–10689.
23. Sohn, C.-H., Park, S.P., Choi, S.H., Park, S.-H., Kim, S., et al. (2015). MRI molecular imaging using GLUT1 antibody-Fe3O4 nanoparticles in the hemangioma animal model for differentiating infantile hemangioma from vascular malformation. *Nanomed. Nanotechnol. Biol. Med*; 11:127–135.
24. Yang, M., Gao, L., Liu, K., Luo, C., Wang, Y., et al. (2015). Characterization of Fe3O4/SiO2/Gd2O(CO3)2 core/shell/shell nanoparticles as T1 and T2 dual mode MRI contrast agent. *Talanta*; 131:661–665.
25. Gijs, M.A., Lacharme, F., Lehmann, U. (2010). Microfluidic applications of magnetic particles for biological analysis and catalysis. *Chem. Rev*; 110:1518–1563.

26. Plouffe, B.D., Murthy, S.K., Lewis, L.H. (2014). Fundamentals and application of magnetic particles in cell isolation and enrichment. *A Rev. Rep. Prog. Phys*; 78:016601.
27. Reddy, L.H., Arias, J.L., Nicolas, J., Couvreur, P. (2012). Magnetic nanoparticles: design and characterization, toxicity and biocompatibility, pharmaceutical and bio-medical applications. *Chem. Rev*; 112:5818–5878.
28. Meidanchi, A., Akhavan, O., Khoei, S., Shokri, A.A., Hajikarimi, Z., et al. (2015). ZnFe2O4 nanoparticles as radiosensitizers in radiotherapy of human prostate cancer cells. *Mater. Sci. Eng. C*; 46:394–399.
29. Obaidat, L.M., Issa, B., Haik, Y. (2015). Magnetic properties of magnetic nanoparticles for efficient hyperthermia. *Nanomaterials*; 5:63–89.
30. Xiang, D., Shigdar, S., Qiao, G., Wang, T., Kouzani, A.Z., et al. (2015). Nucleic acid aptamer-guided cancer therapeutics and diagnostics: the next generation of cancer medicine. *Theranostics*; 5:23–42.
31. Wu, W., Wu, Z., Yu, T., Changzhong, J., Kim, W.-S. (2015). Recent progress on magnetic iron oxide nanoparticles: synthesis, surface functional strategies and biomedical applications. *Sci. Technol. Adv. Mater*; 16:23501.
32. Spirou, S.V., Basini, M., Lascialfari, A., Sangregorio, C., Innocenti, (C. 2018). Magnetic hyperthermia and radiation therapy: radiobiological principles and current practice. *Nanomaterials*; 8:1–22.
33. Beveridge, J.S., Stephens, J.R., Williams, M.E. (2011). The use of magnetic nanoparticles in analytical chemistry. *Annu. Rev. Anal. Chem*; 4:251–273.
34. Xu, Y., Wang, E. (2012). Electrochemical biosensors based on magnetic micro/ nanoparticles. *Electrochim. Acta*; 84:62–73.
35. Carregal-Romero, S., Caballero-Diaz, E., Beqa, L., Abdelmonem, A.M., Ochs, M., et al. (2013). Muliplexed sensing and imaging with colloidal nano- and microparticles. *Annu. Rev. Anal. Chem*; 6:53–81.
36. Iranifam, M. (2013). Analytical applications of chemiluminescence-detection systems assisted by magnetic microparticles and nanoparticles. *Trends Anal. Chem*; 51:51–70.
37. Lee, J.-H., Kim, J.W., Levy, M., Kao, A., Noh, S.H., Bozovic, D., Cheon, J. Magnetic. (2014). nanoparticles for ultrafast mechanical control of inner ear hair cells. *ACS Nano*; 8:6590–6598.
38. Rocha-Santos, T.A.P. (2014). Sensors and biosensors based on magnetic nanoparticles. *TrAC Trends Anal. Chem*; 62:28–36.
39. Abbas, M., Islam, M.N., Rao, B.P., Abdel-Hamed, M.O., Kim, C. (2015). Facile one-pot chemical approach for synthesis of monodisperse chain-like superparamagnetic maghemite (γ-Fe2O3) nanoparticles. *J. Ind. Eng. Chem*; 31:43–46.
40. Maksoud, M.I.A., S.G. El-Sayyad, Ashour, A.H., El-Batal, A.I., Abd-Elmonem, M.S., Hendawy, H.A.M., et al. (2018). Synthesis and characterization of metals-substituted cobalt ferrite [Co (1−x)] M xFe2O4; (M = Zn, Cu, Mn; x = 0,05)] nanoparticles as antimicrobial agents and sensors for Anagrelide determination in biological samples. *Mater. Sci. Eng. C*; 92:644–656.
41. Lu, A.H., Salabas, E.L., Schüth, F. (2007). Magnetic nanoparticles: synthesis, protection, functionalization, and application. Angewandte *Chemie International Edition*; 46:1222-1244.
42. Yoon, S., Krishnan, K.M. (2011). Temperature dependence of magnetic anisotropy constant in manganese ferrite nanoparticles at low temperature. *J. Appl. Phys*; 109:07B534.
43. Ling, D., Lee, N., Hyeon, T. (2015). Chemical synthesis and assembly of uniformly sized iron oxide nanoparticles for medical applications. *Acc. Chem. Res*; 48:1276–1285.
44. Park, J., An, K., Hwang, Y., Park, J.-G., Noh, H.-J., et al. (2004). Ultra-large-scale syntheses of monodisperse nanocrystals. *Nat. Mater*; 3:891–895.
45. Suleiman, J.S., Hu, B., Peng, H., Huang, C. (2009). Separation/preconcentration of trace amounts of Cr, Cu and Pb in environmental samples by magnetic solid-phase extraction with Bismuthiol-II-immobilized magnetic nanoparticles and their determination by ICP-OES. *Talanta*; 77:1579–1583.
46. Akbarzadeh, A., Samiei, M., Davaran, S. (2012). Magnetic nanoparticles: preparation, physical properties, and applications in biomedicine. *Nanoscale Res. Lett*; 7:144–156.
47. Rahimi, R., Maleki, A., Maleki, S., Morsali, A., Rahimi, M.J. (2014). Synthesis and characterization of magnetic dichromate hybrid nanomaterials with triphenylphosphine surface modified iron oxide nanoparticles (Fe3O4@SiO2@PPh3@Cr2O7 2−). *Solid State Sci*; 28:9–13.
48. Issa, B., Obaidat, I.M., Albiss, B.A., Haik, Y. (2013). Magnetic nanoparticles: surface effects and properties related to biomedicine applications, *International Journal of Molecular Sciences*; 14:21266-21305.
49. Pisane, K.L., Despeaux, E.C., Seehra, M.S. (2015). Magnetic relaxation and correlating effective magnetic moment with particle size distribution in maghemite nanoparticles. *Journal of Magnetism and Magnetic Materials*; 384:148-154.
50. Ruta, S., Chantrell, R., Hovorka, O. (2015). Unified model of hyperthermia via hysteresis heating in systems of interacting magnetic nanoparticles. *Scientific Reports*; 5:9090, 1-7.
51. Mathew, D.S., Juang, R.-S. (2007). An overview of the structure and magnetism of spinel ferrite nanoparticles and their synthesis in microemulsions. *Chemical engineering journal*; 129:51-65.
52. Kusigerski, V., Illes, E., Blanusa, J., Gyergyek, S., Boskovic, M., et al. (2019). Magnetic properties and heating efficacy of magnesium doped magnetite nanoparticles obtained by co-precipitation method. *J. Magn. Magn. Mater*; 475:470–478.
53. Marinca, T.F., Chicinaş, I., Isnard, O. (2013). Structural and magnetic properties of the copper ferrite obtained by reactive milling and heat treatment. *Ceram. Int*; 39:4179–4186.
54. Cullity, B.D., Graham, C.D. (2009). Introduction to Magnetic Materials. A John Wiley & Sons, Inc., Hoboken, New Jersey: 361.
55. Cullity, B.D., Graham, C.D. (2009). Introduction to magnetic materials. Mater. Today; 12:45.
56. Zaki, H.M., Al-Heniti, S.H., Hashhash, A. (2016). Effect of Al3+ ion addition on the magnetic properties of cobalt ferrite at moderate and low temperatures. *J. Magn. Magn. Mater*; 401:1027–1032.
57. Zi, Z., Sun, Y., Zhu, X., Yang, Z., Dai, J., et al. (2009). Synthesis and magnetic properties of CoFe2O4 ferrite nanoparticles. *J. Magn. Magn. Mater*; 321:1251–1255.
58. Kefeni, K.K., Msagati, T.M., Mamba, B.B. (2015). Synthesis and characterization of magnetic nanoparticles and study their removal capacity of metals from acid mine drainage. *Chem. Eng. J*. 2015; 276:222–231.
59. Nabiyouni, G., Julaee, M., Ghanbari, D., Aliabadi, P.C., Safaie, N. (2015). Room temperature synthesis and

magnetic property studies of Fe3O4 nanoparticles prepared by a simple precipitation method. *J. Ind. Eng. Chem*; 21:599–603.

60. Thakur, S., Rai, R., Sharma, S. (2015). Structural characterization and magnetic study of NiFexO4 synthesized by co-precipitation method. *Mater. Lett*; 139:368–372.
61. Xing, Y., Jin, Y.-Y., Si, J.-C., Peng, M.-L., Wang, X.-F., et al. (2015). Controllable synthesis and characterization of Fe3O4/Au composite nanoparticles. *J. Magn. Magn. Mater*; 380:150–156.
62. Ge, Q., Su, J., Chung, T.-S., Amy, G. (2011). Hydrophilic superparamagnetic nanoparticles: synthesis, characterization, and performance in forward osmosis processes. *Ind. Eng. Chem. Res*; 50:382–388.
63. Darezereshki, E., Bakhtiari, F., Alizadeh, M., Behrad vakylabad, A., Ranjbar, M. (2012). Direct thermal decomposition synthesis and characterization of hematite (αFe2O3) nanoparticles. *Mater. Sci. Semicond. Process*; 15:91–97.
64. Fantechi, E., Innocenti, C., Albino, M., Lottini, E., Sangregorio, C. (2015). Influence of cobalt doping on the hyperthermic efficiency of magnetite nanoparticles. *J. Magn. Magn. Mater*; 380: 365–371.
65. Zakiyah, L.B., Saion, E., Al-Hada, N.M., Gharibshahi, E., Salem, A., et al. (2015). Up-scalable synthesis of size-controlled copper ferrite nanocrystals by thermal treatment method, *Mater. Sci. Semicond. Process*. 40: 564–569.
66. Nemati, A., Shadpour, S., Khalafbeygi, H., Barkhi, M. (2014). Hydrothermal synthesis and size control of Fe3O4 nanoparticles in the presence of 2,2',2",2" ′-(ethane-1,2-diylbis(azanetriyl)) tetraacetohydrazide, synth. React. Inorganic, Met. *Nano-Metal Chem*; 44:1161–1165.
67. Tadic, M., Panjan, M., Damnjanovic, V., Milosevic, I. (2014). Magnetic properties of hematite (α-Fe2O3) nanoparticles prepared by hydrothermal synthesis method. *Appl, Surf. Sci*; 320:183–187.
68. Ding, Z., Wang, W., Zhang, Y., Li, F., Liu, J.P. (2015). Synthesis, characterization and adsorption capability for Congo red of CoFe2O4 ferrite nanoparticles. *J. Alloy. Comp*; 640:362–370.
69. Cruz, M.M., Ferreira, L.P., Ramos, J., Mendo, S.G., Alves, A.F., et al. (2017). Enhanced magnetic hyperthermia of CoFe2O4 and MnFe2O4 nanoparticles. *J. Alloy. Comp*; 703:370–380.
70. Tian, Y., Yu, B., Li, X., Li, K. (2011). Facile solvothermal synthesis of monodisperse Fe3O4 nanocrystals with precise size control of one nanometre as potential MRI contrast agent. *J. Mater. Chem*; 21:2476–2481.
71. Ameer, S., Gul, I.H., Mujahid, M. (2015). Ultra-low permittivity/loss CoFe2O4 and CoFe2O4–rGO nanohybrids by novel 1-hexanol assisted solvothermal process. *J. Alloy. Comp*; 642:78–82.
72. Tao, B., Zhang, Q., Liu, Z., Geng, B. (2012). Cooperative effect of pH value and anions on single-crystalline hexagonal and circular α-Fe2O3 nanorings. *Mater. Chem. Phys*; 136:604–612.
73. Shen, C.Q., Ji, H.N., Wu, J., Zhu, N., Niu, J.Q., et al. (2018). Synthesis and characterization of mnzn ferrite nanoparticles for biomedical applications. Supercond. Electromagn. Devices, ASEMD :1–2.
74. Larumbe, S., Perez-Landazabal, J.I., Pastor, J.M., Gomez-Polo, C. (2012). Sol-gel NiFe2O4 nanoparticles: effect of the silica coating. *J. Appl. Phys*; 111:103911–103918.
75. Avazpour, L., Zandi khajeh, M.A., Toroghinejad, M.R., Shokrollahi, H. (2015). Synthesis of single-phase cobalt ferrite nanoparticles via a novel EDTA/EG precursor-based route and their magnetic properties. *J. Alloy. Comp* ;637: 497–503.
76. Masthoff, I.C., Kraken, M., Mauch, D., Menzel, D., Munevar, J.A., et al. (2014). Study of the growth process of magnetic nanoparticles obtained via the non-aqueous sol–gel method. *J. Mater. Sci*; 49:4705–4714.
77. Elayakumar, K., Dinesh, A., Manikandan, A., Palanivelu, M., Kavitha, G., et al. (2019). Structural, morphological, enhanced magnetic properties and antibacterial bio-medical activity of rare earth element (REE) cerium (Ce3+) doped CoFe2O4 nanoparticles. *J. Magn. Magn. Mater*; 476:157–165.
78. Abid, A.D., Kanematsu, M., Young, T.M., Kennedy, I.M. (2013). Arsenic removal from water using flame-synthesized iron oxide nanoparticles with variable oxidation states. *Aerosol Sci. Technol*.,47:169–176.
79. Hassanjani-Roshan, A., Vaezi, M.R., Shokuhfar, A., Rajabali, Z. (2011). Synthesis of iron oxide nanoparticles via sonochemical method and their characterization. Particuology; 9:95–99.
80. Zhang, S., Zhang, Y., Wang, Y., Liu, S., Deng, Y. (2012). Sonochemical formation of iron oxide nanoparticles in ionic liquids for magnetic liquid marble. *Phys. Chem. Chem. Phys*; 14:5132–5138.
81. Xu, H., Zeiger, B.W., Suslick, K.S. (2013). Sonochemical synthesis of nanomaterials. *Chem. Soc. Rev*; 42:2555–2567.
82. Zhu, S., Guo, J., Dong, J., Cui, Z., Lu, T., et al. (2013). Sonochemical fabrication of Fe3O4 nanoparticles on reduced graphene oxide for biosensors. *Ultrason. Sonochem*; 20:872–880.
83. Zhang, D., Zhang, X., Ni, X., Song, J., H. Zheng, H. (2006). Low-temperature fabrication of MnFe2O4 octahedrons: magnetic and electrochemical properties. *Chem. Phys. Lett*; 426:120–123.
84. Amendola, V., Riello, P., Meneghetti, M. (2011). Magnetic nanoparticles of iron carbide, iron oxide iron@iron oxide, and metal iron synthesized by laser ablation in organic solvents. *J. Phys. Chem. C*; 115:5140–5146.
85. Franzel, L., Bertino, M.F., Huba, Z.J., Carpenter, E.E. (2012). Synthesis of magnetic nanoparticles by pulsed laser ablation. *Appl. Surf. Sci*; 261:332–336.
86. Konicki, W., Sibera, D., Mijowska, E., Lendzion-Bieluń, Z., Narkiewicz, U. (2013). Equilibrium and kinetic studies on acid dye Acid Red 88 adsorption by magnetic ZnFe2O4 spinel ferrite nanoparticles. *J. Colloid Interface Sci*; 398:152–160.
87. Dandia, A., Parewa, V., Gupta, S.L., Sharma, A., Rathore, K.S., et al. (2015). Microwaveassisted Fe3O4 nanoparticles catalyzed synthesis of chromeno [1,6] naphthyridines in aqueous media. *Catal. Commun*; 61:88–91.
88. Mondal, A.K., Chen, S., Su, D., Kretschmer, K., Liu, H., et al. (2015). Microwave synthesis of α-Fe2O3 nanoparticles and their lithium storage properties: a comparative study. *J. Alloy. Comp*; 648:732–739.
89. Zeng, S., Duan, S., Tang, R., Li, L., Liu, C., et al. (2014). Magnetically separable Ni0.6Fe2.4O4 nanoparticles as an effective adsorbent for dye removal: synthesis and study on the kinetic and thermodynamic behaviors for dye adsorption. *Chem. Eng. J*; 258:218–228.
90. Foroughi, F., Hassanzadeh-Tabrizi, S.A., Amighian, J., Saffar-Teluri, A. (2015). A designed magnetic CoFe2O4–hydroxyapatite core–shell nanocomposite for Zn (II) removal with high efficiency. Ceram. Int; 41:6844–6850.
91. Rashad, M.M., Soltan, S., Ramadan, A.A., Bekheet, M.F., Rayan, D.A. (2015). Investigation of the structural, optical

and magnetic properties of CuO/CuFe2O4 nanocomposites synthesized via simple microemulsion method. *Ceram. Int*; 41:12237–12245.

92. Flores-Arias, Y., Azquez-Victorio, G.V., Ortega-Zempoalteca, R., Acevedo-Salas, U., Ammar, S., et al. (2015). Magnetic phase transitions in ferrite nanoparticles characterized by electron spin resonance. *J. Appl. Phys*; 117(17): 17A503.
93. Gaudisson, T., Beji, Z., Herbst, F., Nowak, S., Ammar, S., et al. (2015). Ultrafine grained high density manganese zinc ferrite produced using polyol process assisted by Spark Plasma Sintering. *J. Magn. Magn. Mater*; 387:90–95.
94. Solano, E., Yáñez, R., Ricart, S., Ros, J. (2015). New approach towards the polyol route to fabricate MFe2O4 magnetic nanoparticles: the use of MCl2 and Fe(acac)3 as chemical precursors. J. Magn. Magn. Mater; 382:380–385.
95. Fajaroh, F., Setyawan, H., Widiyastuti, W., Winardi, S. (2012). Synthesis of magnetite nanoparticles by surfactant-free electrochemical method in an aqueous system. *Adv. Powder Technol*; 23:328–333.
96. Galindo, R., Mazario, E., Gutiérrez, S., Morales, M.P., Herrasti, P. (2012). Electrochemical synthesis of NiFe2O4 nanoparticles: characterization and their catalytic applications. J. Alloy. Comp; 536: S241–S244.
97. Mazario, E., Morales, M.P., Galindo, R., Herrasti, P., Menendez, N. (2012). Influence of the temperature in the electrochemical synthesis of cobalt ferrites nanoparticles. *J. Alloy. Comp*; 536: S222–S225.
98. Karimzadeh, I., Aghazadeh, M., Reza, M., Norouzi, P. (2017). Saccharide-coated superparamagnetic Fe3O4 nanoparticles (SPIONs) for biomedical applications: an ef ficient and scalable route for preparation and in situ surface coating through cathodic electrochemical deposition (CED). *Mater. Lett* ;189:290–294.
99. Lemine, O.M. (2009). Microstructural characterisation of nanoparticles using, XRD line profiles analysis, FE-SEM and FT-IR. *Superlattice Microstruct*; 45:576–582.
100. Safarik, I., Horska, K., Pospiskova, K., Maderova, Z., Safarikova, M. (2013). Microwaveassisted synthesis of magnetically responsive composite materials. *IEEE Trans. Magn*; 49(1):213-218.
101. Wang, F., Qin, X.F., Meng, Y.F., Guo, Z.L., Yang, L.X., et al. (2013). Hydrothermal synthesis and characterization of α-Fe2O3 nanoparticles. *Mater. Sci. Semicond. Process*; 16:802–806.
102. Sulaiman, N.H., Ghazali, M.J., Yunas, J., Rajabi, A., Majlis, B.Y., et al. (2018). Synthesis and characterization of CaFe2O4 nanoparticles via co-precipitation and autocombustion methods. *Ceram. Int*; 44:46–50.
103. Dong, H., Du, S.-R., Zheng, X.-Y., Lyu, G.-M., Sun, L.-D., et al. (2015). Lanthanide nanoparticles: from design toward bioimaging and therapy. *Chem. Rev*; 115:10725–10815.
104. Sánchez, J., Cortés-Hernández, D.A., Escobedo-Bocardo, J.C., Almanza-Robles, J.M., Reyes-Rodríguez, P.Y., et al. (2017). Synthesis of MnxGa1−xFe2O4 magnetic nanoparticles by thermal decomposition method for medical diagnosis applications. J. Magn. Magn. Mater; 427:272–275.
105. Reyes-Rodríguez, P.Y., Cortés-Hernández, D.A., Escobedo-Bocardo, J.C., Almanza-Robles, J.M., Sánchez, J., et al. (2018). Synthesis and Study of Structural and Magnetic Properties of Mg1-xZnxFe2O4 (X= 0-0,9). *Matéria, Rio Janeiro*: 1–4.
106. Laurent, S., Forge, D., Port, M., Roch, A., Robic, C., et al. (2008). Magnetic iron oxide nanoparticles: synthesis, stabilization, vectorization, physicochemical characterizations, and biological applications. *Chem. Rev*; 108:2064–2110.
107. Palma, S.I.C.J., Marciello, M., Carvalho, A., Veintemillas-Verdaguer, S., del P. Morales, M., et al. (2015). Effects of phase transfer ligands on monodisperse iron oxide magnetic nanoparticles. *J. Colloid Interface Sci*; 437:147–155.
108. Fantechi, E., Campo, G., Carta, D., Corrias, A., de Julián Fernández, C., et al. (2012). Exploring the effect of Co doping in fine maghemite nanoparticles. *J. Phys. Chem. C*; 116:8261–8270.
109. Monfared, A.H., Zamanian, A., Sharifi, I., Mozafari, M. (2019). Reversible multistimuli-responsive manganese–zinc ferrite/P(NIPAAM-AAc-AAm) core-shell nanoparticles: a programmed ferrogel system. *Mater. Chem. Phys*; 226:44–50.
110. Amiri, S., Shokrollahi, H. (2013). Magnetic and structural properties of RE doped Co ferrite (RE = Nd, Eu, Gd) nanoparticles synthesized by co-precipitation. *J. Magn. Magn. Mater*; 345:18–23.
111. Amiri, S., Shokrollahi, H. (2013). The role of cobalt ferrite magnetic nanoparticles in medical science. Mater. Sci. Eng. C; 33:1–8.
112. Lin, Q., Xu, J., Yang, F., Lin, J., Yang, H., He, Y. (2018). Magnetic and mössbauer spectroscopy studies of zinc-substituted cobalt ferrites prepared by the sol-gel method. *Materials*; 11:1–12.
113. Karimi, Z., Mohammadifar, Y., Shokrollahi, H., Asl, S.K., Yousefi, G., et al. (2014). Magnetic and structural properties of nano sized Dy-doped cobalt ferrite synthesized by co-precipitation. *J. Magn. Magn. Mater*; 361:150–156.
114. Gharibshahian, M., Mirzaee, O., Nourbakhsh, M. (2017). Evaluation of superparamagnetic and biocompatible properties of mesoporous silica coated cobalt ferrite nanoparticles synthesized via microwave modified Pechini method. *J. Magn. Magn. Mater*; 425:48–56.
115. Chinnasamy, C.N., Jeyadevan, B., Shinoda, K., Tohji, K., Djayaprawira, D.J., Takahashi, M., et al. (2003). Unusually high coercivity and critical single-domain size of nearly monodispersed CoFe2O4 nanoparticles. *Appl. Phys. Lett*; 83:2862–2864.
116. Ponce, A.S., Chagas, E.F., Prado, R.J., Fernandes, C.H.M., Terezo, A.J., et al. (2013). High coercivity induced by mechanical milling in cobalt ferrite powders. J. Magn. *Magn. Mater*; 344:182–187.
117. Iqbal, S., Fakhar-e-Alam, M., Atif, M., Amin, N., Alimgeer, K.S., et al. (2019). Structural, morphological, antimicrobial, and in vitro photodynamic therapeutic assessments of novel Zn+2-substituted cobalt ferrite nanoparticles. *Results Phys*; 15:102529.
118. Kim, J., Lee, H.S., Lee, M., Lee, S.H. Comparative magneto-optical investigation of dd charge-transfer transitions in Fe3O4, CoFe2O4, and NiFe2O4. *J. Appl. Phys 2002*; 91:9974–9976.
119. Paulsen, J., Ring, A., Lo, C.C., Snyderb, J., Jiles, J.A.D.C. (2005). Manganese-substituted cobalt ferrite magnetostrictive materials for magnetic stress sensor applications. *J. Appl. Phys*, 97:44502–44505.
120. Zhao, J., Deng, M., Zeng, J., Huang, Z., Yin, G., et al. (2012). Preparation of Fe3O4 and CoFe2O4 nanoparticles with cellular compatibility via the histidine assistance. Colloids Surfaces a Physicochem. *Eng. Asp*; 401:54–60.
121. Meng, X., Li, H., Chen, J., Mei, L., Wang, K., et al. (2009). Mössbauer study of cobalt ferrite nanocrystals substituted with rare-earth Y3+ ions. *J. Magn. Magn. Mater*; 321:1155–1158.

122. Liu, Y., Jiang, W., Xu, L., Yang, X., Li, F. (2009). Decoration of carbon nanotubes with nearly monodisperse MIIFe2O4 (MFe2O4, M = Fe, Co, Ni) nanoparticles. *Mater. Lett*; 63:2526–2528.
123. Hwang, D.W., Ko, H.Y., Lee, J.H., Kang, H., Ryu, S.H., et al. (2010). A nucleolin-targeted multimodal nanoparticle imaging probe for tracking cancer cells using an aptamer. *J. Nucl. Med*; 51:98–105.
124. Wu, H., Liu, G., Wang, X., Zhang, J., Chen, Y., et al. (2011). Solvothermal synthesis of cobalt ferrite nanoparticles loaded on multiwalled carbon nanotubes for magnetic resonance imaging and drug delivery. Acta Biomater; 7:3496–3504.
125. Balakrishnan, S., Bonder, M. (2009). Particle size effect on phase and magnetic properties of polymer-coated magnetic nanoparticles. *J. Magn. Magn. Mater*; 321:117-122.
126. Psimadas, D., Baldi, G., Ravagli, C., Comes, F.M., Locatelli, C., et al. (2014). Comparison of the magnetic, radiolabeling, hyperthermic and biodistribution properties of hybrid nanoparticles bearing CoFe2O4 and Fe3O4 metal cores. *Nanotechnology*; 25:25101.
127. Georgiadou, V., Tangoulis, V., Arvanitidis, I., Kalogirou, O., Dendrinou-Samara, C. (2015). Unveiling the physicochemical features of CoFe2O4 nanoparticles synthesized via a variant hydrothermal method: NMR relaxometric properties. *J. Phys. Chem. C*; 119:8336–8348.
128. Demirci, E., Manna, P.K., Wroczynskyj, Y., Aktürk, S., van Lierop, J. (2018). Lanthanum ion substituted cobalt ferrite nanoparticles and their hyperthermia efficiency. *J. Magn. Magn. Mater*; 458:253–260.
129. Karimi, Z., Karimi, L., Shokrollahi, H. (2013). Nano-magnetic particles used in biomedicine: core and coating materials. *Mater. Sci. Eng. C*; 33:2465–2475.
130. Baldi, G., Bonacchi, D., Innocenti, C., Lorenzi, G., Sangregorio, C. (2007). Cobalt ferrite nanoparticles: the control of the particle size and surface state and their effects on magnetic properties. *J. Magn. Magn. Mater*; 311:10–16.
131. Albino, M., Fantechi, E., Innocenti, C., López-Ortega, A., Bonanni, V., et al. (2019). Role of Zn2+ substitution on the magnetic, hyperthermic, and relaxometric properties of cobalt ferrite nanoparticles. *J. Phys. Chem. C*; 123:6148–6157.
132. Duong, G.V., Hanh, N., Linh, D.V., Groessinger, R., Weinberger, P., S. et al. (2007). Monodispersed nanocrystalline Co1–xZnxFe2O4 particles by forced hydrolysis: Synthesis and characterization. *J. Magn. Magn. Mater*; 311:46–50.
133. Almessiere, M.A., Slimani, Y., Sertkol, M., Khan, F.A., Nawaz, M., et al. (2019). Ce–Nd Co-substituted nanospinel cobalt ferrites: an investigation of their structural, magnetic, optical, and apoptotic properties. *Ceram. Int*; 45:16147–16156.
134. Deepak, F.L., Bañobre-López, M., Carbó-Argibay, E., Cerqueira, M.F., PiñeiroRedondo, Y., et al. (2015). A systematic study of the structural and magnetic properties of Mn-, Co-, and Ni-doped colloidal magnetite nanoparticles. *J. Phys. Chem. C*; 119:11947–11957.
135. Gao, L., Wu, J., Lyle, S., Zehr, K., Cao, L., et al. (2008). Magnetite nanoparticle-linked immunosorbent assay. *J. Phys. Chem. C*; 112:17357–17361.
136. Grumezescu, A.M., Andronescu, E., Ficai, A., Grumezescu, V., Bleotu, C., et al. (2013). Biocompatible magnetic hollow silica microspheres for drug delivery. *Curr. Org. Chem*; 17:1029–1033.
137. Wang, C.Z. (2014). Preparation and characterization of surfacefunctionalization of silicacoated magnetite nanoparticles for drug delivery. *Nano*; 9:1–8.
138. Fard, A.E., Zarepour, A., Zarrabi, A., Shanei, A., Salehi, H., et al. (2015). Synergistic effect of the combination of triethylene-glycol modified Fe3O4 nanoparticles and ultrasound wave on MCF-7 cells. *J. Magn. Magn. Mater*; 394:44–49.
139. Vallabani, N.V.S., Singh, S. (2018). Recent advances and future prospects of iron oxide nanoparticles in biomedicine and diagnostics. *Biotech*; 8:1–23.
140. Orlando, T., Albino, M., Orsini, F., Innocenti, C., Basini, M., et al. (2016). On the magnetic anisotropy and nuclear relaxivity effects of Co and Ni doping in iron oxide nanoparticles. *J. Appl. Phys*; 119:134301.
141. de Mello, L.B., Varanda, L.C., Sigoli, F.A., Mazali, I.O. (2019). Co-precipitation synthesis of (Zn-Mn)-co-doped magnetite nanoparticles and their application in magnetic hyperthermia. *J. Alloy. Comp*; 779:698–705.
142. Saha, P., Rakshit, R., Mandal, K. (2019). Enhanced magnetic properties of Zn doped Fe3O4 nano hollow spheres for better bio-medical applications. *J. Magn. Magn. Mater*; 475:130–136.
143. Mozaffari, M., Shatooti, S., Jafarzadeh, M., Niyaifar, M., Aftabi, A., et al. (2015). Synthesis of Zn2+ substituted maghemite nanoparticles and investigation of their structural and magnetic properties. J. *Magn. Magn. Mater* 382:366–375.
144. Teja, A., Koh, P.Y. (2009). Synthesis, properties, and applications of magnetic iron oxide nanoparticles. Prog. Cryst. *Growth Charact. Mater*; 55:22–45.
145. Sutradhar, S., Das, S., Roychowdhury, A., Das, D., Chakrabarti, P.K. (2015). Magnetic property, Mössbauer spectroscopy and microwave reflection loss of maghemite nanoparticles (γ-Fe2O3) encapsulated in carbon nanotubes. *Mater. Sci. Eng. B*; 196:44–52.
146. Gilchrist, R.K., Medal, R., Shorey, W.D., Hanselman, R.C., Parrott, J.C., et al. (1957). Selective inductive heating of lymph nodes. *Annals of Surgery*; 146:596–606.
147. Kluchova, K., Zboril, R., Tucek, J., Pecova, M., Zajoncova, L., et al. (2009). Superparamagnetic maghemite nanoparticles from solid-state synthesis – their functionalization towards peroral MRI contrast agent and magnetic carrier for trypsin immobilization. *Biomaterials*; 30:2855–2863.
148. Stagi, L., De Toro, J.A., Ardu, A., Cannas, C., Casu, A., et al. (2014). Surface effects under visible irradiation and heat treatment on the phase stability of γFe2O3 nanoparticles and γ-Fe2O3 −SiO2 core–shell nanostructures. *J. Phys. Chem. C*; 118:2857–2866.
149. Sharifi, I., Shokrollahi, H., Amiri, S. (2012). Ferrite-based magnetic nanofluids used in hyperthermia applications. *J. Magn. Magn. Mater*; 324:903–915.
150. Ahmed, M.A., Okasha, N., El-Dek, S.I. (2008). Preparation and characterization of nanometric Mn ferrite via different methods. *Nanotechnology*; 19:1–6.
151. Sam, S., Nesaraj, A.S. (2011). Preparation of MnFe2O4 nanoceramic particles by soft chemical routes. *Int. J. Appl. Sci. Eng*; 9:223–239.
152. Soleimani, R., Soleimani, M., Godarzi, M.G. (2011). Preparation of soft manganese ferrite and inventional of its magnetic properties and Mn55 nuclear magnetic resonance. *J. Fusion Energy*; 30:338–341.
153. Kadam, R.H., Desai, K., Shinde, V.S., Hashim, M., Shirsath, S.E. (2016). Influence of Gd3+ ion substitution on the MnCrFeO4 for their nanoparticle shape formation and magnetic properties. *J. Alloy. Comp*; 657:487–494.

154. Kim, D.-H., Zeng, H., Ng, T.C., Brazel, C.S. (2009). T1 and T2 relaxivities of succimer-coated MFe2 3+O4 (M=Mn2+, Fe2+ and Co2+) inverse spinel ferrites for potential use as phase-contrast agents in medical MRI. *J. Magn. Magn. Mater*; 321:3899–3904.
155. Kim, D.-H., Nikles, D.E., Brazel, C.S. (2010). Synthesis and characterization of multifunctional chitosan-MnFe2O4 nanoparticles for magnetic hyperthermia and drug delivery. *Materials*; 3:4051.
156. Lee, J.-H., Jang, J., Choi, J., Moon, S.H., Noh, S., et al. (2011). Exchange-coupled magnetic nanoparticles for efficient heat induction. *Nat. Nanotechnol*; 6:418–422.
157. Hajalilou, A., Hashim, M., Ebrahimi-Kahrizsangi, R., Mohamed kamari, H., Sarami, N. (2014). Synthesis and structural characterization of nano-sized nickel ferrite obtained by mechanochemical process. *Ceram. Int*; 40:5881–5887.
158. Ahmad, T., Rhee, I., Hong, S., Chang, Y., Lee, J. (2011). NiFe2O4 nanoparticles as contrast agents for magnetic resonance imaging. *J. Nanosci. Nanotechnol*; 11:5645–5650.
159. Bae, S., Lee, S.W., Takemura, Y. (2006). Applications of NiFe2O4 nanoparticles for a hyperthermia agent in biomedicine. *Appl. Phys. Lett*; 89:252503.
160. Phadatare, M.R., Khot, V.M., Salunkhe, A.B., Thorat, N.D., Pawar, S.H. (2012). Studies on polyethylene glycol coating on NiFe2O4 nanoparticles for biomedical applications. *J. Magn. Magn. Mater*; 324:770–772.
161. Shanmugavani, A., Kalai Selvan, R., Layek, S., Sanjeeviraja, C. (2014). Size dependent electrical and magnetic properties of ZnFe2O4 nanoparticles synthesized by the combustion method: comparison between aspartic acid and glycine as fuels. *J. Magn. Magn. Mater*; 354:363–371.
162. Bahhar, S., Lemziouka, H., Boutahar, A., Bioud, H., Lassri, H., et al. (2019). Influence of La 3+ site substitution on the structural, magnetic and magnetocaloric properties of ZnFe2−x Lax O4 (x = 0.00, 0.001, 0.005 and 0.01) spinel zinc ferrites. *Chem. Phys. Lett*; 716:186–191.
163. Kombaiah, K., Vijaya, J.J., Kennedy, L.J., Bououdina, M. (2016). Studies on the microwave assisted and conventional combustion synthesis of Hibiscus rosa-sinensis plant extract based ZnFe2O4 nanoparticles and their optical and magnetic properties. *Ceram. Int*; 42:2741–2749.
164. Hong, N.H., Raghavender, A.T., Ciftja, O., Phan, M.H., Stojak, K., et al. (2013). Ferrite nanoparticles for future heart diagnostics, *Appl. Phys. A*; 112:323–327.
165. Margabandhu, M., Sendhilnathan, S., Senthilkumar, S., Gajalakshmi, D. (2016). Investigation of structural, morphological, magnetic properties and biomedical applications of Cu2+ substituted uncoated cobalt ferrite nanoparticles. Braz. *Arch. Biol. Technol*.; 59:1–10.
166. Amiri, M., Salavati-Niasari, M., Akbari, A. (2019). Magnetic nanocarriers: evolution of spinel ferrites for medical applications. *Adv. Colloid Interface Sci*; 265:29–44.
167. Song, Q., Zhang, Z.J. (2004). Shape control and associated magnetic properties of spinel cobalt ferrite nanocrystals. *J. Am. Chem. Soc*; 126:6164–6168.
168. Salazar-Alvarez, G., Qin, J., Sepelak, V., Bergmann, I., Vasilakaki, M., et al. (2008). Cubic versus spherical magnetic nanoparticles: the role of surface anisotropy. *Am. Chem. Soc*; 130:13234.
169. Krishnan, K.M. (2010). Biomedical Nanomagnetics, A spin through possibilities in imaging, diagnostics, and therapy. *IEEE Trans. Magn*; 46:2523–2558.
170. Jun, Y., Huh, Y.M., Choi, J., Lee, J.H., Song, H.T., et al. (2005). Nanoscale size effect of magnetic nanocrystals and their utilization for cancer diagnosis via magnetic resonance imaging. *J. Am. Chem. Soc*; 127:732–5733.
171. Hjiri, M., Alshammari, S., Besbes, H., Lemine, O.M., Hammad, A.H., et al. (2019). The effect of Ni/Fe ratio on the physical properties of NiFe2O4 nanocomposites. *Mater. Res. Express*; 6:086107.
172. Jun, Y.W., Seo, J.W., Cheon, J. (2008). Nanoscaling laws of magnetic nanoparticles and their applicabilities in biomedical Sciences. *Acc. Chem. Res*; 41:179–189.
173. Hoa, L.T.M., Dung, T.T., Danh, T.M., Duc, N.H., Chien, D.M. (2009). Preparation and characterization of magnetic nanoparticles coated with polyethylene glycol. *J. Phys. Conf. Ser*; 187:12048.
174. Bae, H., Ahmad, T., Rhee, I., Chang, Y., Jin, S.U., et al. (2012). Carbon-coated iron oxide nanoparticles as contrast agents in magnetic resonance imaging. *Nanoscale Res. Lett*; 7:44–48.
175. Parsons, J.G., Lopez, M.L. (2009). Determination of arsenic (III) and arsenic (V) binding to microwave assisted hydrothermal synthetically prepared Fe3O4, Mn3O4, and MnFe2O4 nanoadsorbents. *Microchem. J*; 91:100–106.
176. Zhang, S., Niu, H., Cai, Y., Zhao, X., Shi, Y. (2010). Arsenite and arsenate adsorption on coprecipitated bimetal oxide magnetic nanomaterials, MnFe2O4 and CoFe2O4. *Chem. Eng. J*; 158:599–607.
177. Su, M., Liao, C., Lee, P.H., Li, H., Shih, K. (2017). Formation and leaching behavior of ferrite spinel for cadmium stabilization. *Chem. Eng. Sci*; 158:287–293.
178. Horev-Azaria, L., Kirkpatrick, C.J., Korenstein, R., Marche, P.N., Maimon, O., et al. (2011). Predictive toxicology of cobalt nanoparticles and ions: comparative in vitro study of different cellular models using methods of knowledge discovery from data. *Toxicol. Sci*; 122:489–501.
179. Horev-Azaria, L., Baldi, G., Beno, D., Bonacchi, D., Golla-Schindler, U., et al. (2013). Predictive Toxicology of cobalt ferrite nanoparticles: comparative in-vitro study of different cellular models using methods of knowledge discovery from data. Part, *Fibre Toxicol*; 10:32.
180. Colognato, R., Bonelli, A., Bonacchi, D., Baldi, G., Migliore, L. (2007). Analysis of cobalt ferrite nanoparticles induced genotoxicity on human peripheral lymphocytes: comparison of size and organic grafting-dependent effects. *Nanotoxicology*; 1:301–308.
181. Di Guglielmo, C., López, D.R., De Lapuente, J., Mallafre, J.M.L., Suàrez, M.B. (2010). Embryotoxicity of cobalt ferrite and gold nanoparticles: a first in vitro approach. *Reprod. Toxicol*; 30:271–276.
182. Ahmad, F., Zhou, Y. (2012). Pitfalls and challenges in nanotoxicology: a case of cobalt ferrite (CoFe2O4) nanocomposites. *Chem. Res. Toxicol*; 30:492–507.
183. Dabagh, S., Dini, G. (2019). Synthesis of silica-coated silver-cobalt ferrite nanoparticles for biomedical applications. *J. Supercond. Nov. Magnetism*,
184. Sánchez, J., Cortés-Hernández, D.A., Rodríguez-Reyes, M. (2019). Synthesis of TEG-coated cobalt-gallium ferrites: characterization and evaluation of their magnetic properties for biomedical devices. *J. Alloy. Comp*; 781:1040–1047.
185. Klostergaard, J., Seeney, C.E. (2012). Magnetic nanovectors for drug delivery. *Maturitas*; 73:33–44.
186. Psimadas, D., Baldi, G., Ravagli, C., Bouziotis, P., Xanthopoulos, S., et al. (2012). Preliminary evaluation of a 99mTc labeled hybrid nanoparticle bearing a cobalt ferrite core: in vivo biodistribution. *J. Biomed. Nanotechnol*.8:575-585.

187. Gómez-Lopera, S.A., Plaza, R.C., Delgado, A.V. (2001). Synthesis and characterization of spherical magnetite/biodegradable polymer composite particles. *J. Colloid Interface Sci*; 240:40–47.
188. Sen, T., Bruce, I.J. (2009). Mesoporous silica–magnetite nanocomposites: fabrication, characterisation and applications in biosciences. *Microporous Mesoporous Mater*; 120:246–251.
189. Chen, I.H., Wang, C.-C., Chen, C.-Y. (2010). Fabrication and characterization of magnetic cobalt ferrite/polyacrylonitrile and cobalt ferrite/carbon nanofibers by electrospinning. *Carbon*; 48:604–611.
190. Limaye, M.V., Singh, S.B., Date, S.K., Kothari, D., Reddy, V.R., et al. (2009). High coercivity of oleic acid capped CoFe2O4 Nanoparticles at Room Temperature. *J. Phys. Chem. B*; 113:9070–9076.
191. Jiang, T., Liang, Y., He, Y., Wang, Q. (2015). Activated carbon/NiFe2O4 magnetic composite: a magnetic adsorbent for the adsorption of methyl orange. *J. Environ. Chem. Eng*; 3:1740–1751.
192. Colombo, M., Carregal-Romero, S., Casula, M.F., Gutierrez, L., Morales, M.P., et al. (2012). Biological applications of magnetic nanoparticles. *Chem. Soc. Rev*; 41:4306–4334.
193. Daou, T.J., Greneche, J.M., Pourroy, G., Buathong, S., Derory, A., et al. (2008). Coupling agent effect on magnetic properties of functionalized magnetite-based nanoparticles. *Chem. Mater*; 20:5869–5875.
194. Olsson, R.T., Salazar-Alvarez, G., Hedenqvist, M.S., Gedde, U.W., Lindberg, F., et al. (2005). Controlled synthesis of near-stoichiometric cobalt ferrite nanoparticles. *Chemistry of Materials*; 17:5109-5118.
195. Latham, A.H., Williams, M.E. (2008). Controlling transport and chemical functionality of magnetic nanoparticles. *Accounts of chemical research*; 41:411-420.
196. Yan, Z., Gao, J., Li, Y., Zhang, M., Guo, M. (2015). Hydrothermal synthesis and structure evolution of metal-doped magnesium ferrite from saprolite laterite. *RSC Advances*; 5:92778-92787.
197. El Moussaoui, H., Mahfoud, T., Habouti, S., El Maalam, K., Ali, M.B., et al. (2016). Synthesis and magnetic properties of tin spinel ferrites doped manganese. *Journal of magnetism and magnetic materials*; 405:181-186.
198. Hilpert, S., Verf, V. (1909). Genetische und konstitutive Zusammenhänge in den magnetischen Eigenschaften bei Ferriten und Eisenoxyden, Berichte der deutschen chemischen Gesellschaft; 42:2248-2261.
199. Kato, Y., Takei, T. (1933). Characteristics of metallic oxide magnetic, *Journal of the Institute Eletronic Engineering of Japan*,53:408-412.
200. Albers-Schoenberg, E. (1954). Ferrites for microwave circuits and digital computers, *Journal of Applied Physics*; 25:152-154.
201. Sugimoto, M. (1999). The past, present, and future of ferrites. *Journal of the American Ceramic Society*; 82:269-280.
202. Galvão, W.S., Neto, D., Freire, R.M., Fechine, P.B. (2016). Super-paramagnetic nanoparticles with spinel structure: a review of synthesis and biomedical applications, in: solid state phenomena. *Trans Tech Publ*: 139-176.
203. Hogan, C.L. (1952). The ferromagnetic Faraday effect at microwave frequencies and its applications: the microwave gyrator. *The Bell System Technical Journal*; 31:1- 31.
204. Bobeck, A. (1967). Properties and device applications of magnetic domains in orthoferrites, *The Bell System Technical Journal*; 46:1901-1925.
205. Bobeck, A., Fischer, R., Perneski, A., Remeika, J., Van Uitert, L. (1969). Application of orthoferrites to domain-wall devices. IEEE Transactions on Magnetics; 5:544-553.
206. Dillon Jr., J., Gyorgy, E., Remeika, J. (1969). Photoinduced magnetic anisotropy and optical dichroism in silicon-doped yttrium iron garnet. *Physical Review Letters*; 22:643.
207. Walcott, C., Gould, J.L., Kirschvink, J. (1979). Pigeons have magnets. *Science*; 205:1027-1029.
208. Gould, J.L., Kirschvink, J., Deffeyes, K. (1978). Bees have magnetic remanence. Science; 201:1026-1028.
209. Frankel, R.B., Blakemore, R.P., Wolfe, R.S. (1979). Magnetite in freshwater magnetotactic bacteria. Science; 203:1355-1356.
210. Widder, K.J., Senyei, A.E., Scarpelli, D.G. (1978). Magnetic microspheres: a model system for site specific drug delivery in vivo. Proceedings of the Society for Experimental Biology and Medicine; 158:141-146.
211. Fannin, P. (1991). Measurement of the Neel relaxation of magnetic particles in the frequency range 1 kHz to 160 MHz. *Journal of Physics D: Applied Physics*; 24:76-82.
212. Tartaj, P., del Puerto Morales, M., Veintemillas-Verdaguer, S., González-Carreño, T., Serna, C.J. (2003). The preparation of magnetic nanoparticles for applications in biomedicine. *Journal of Physics D: Applied Physics*; 36: R182-R197.
213. Katoch, G., Rana, G., Singh, M., García-Peñas, A., Bhardwaj, S., et al. (2021). Recent advances in processing, characterizations and biomedical applications of spinel ferrite nanoparticles. *Materials Research Foundations*; 112:62-120.
214. Bragg, W. (1915). The structure of magnetite and the spinels. *Nature*; 95:561-561.
215. Hill, R.J., Craig, J.R., Gibbs, G. (1979). Systematics of the spinel structure type. *Physics and chemistry of minerals*; 4:317-339.
216. Harris, V.G. (2011). Modern microwave ferrites. *IEEE Transactions on Magnetics*; 48:1075-1104.
217. Leal, M.P., Rivera-Fernández, S., Franco, J.M., Pozo, D., Jesús, M., GarcíaMartín, M.L. (2015). Long-circulating PEGylated manganese ferrite nanoparticles for MRI-based molecular imaging. *Nanoscale*,7:2050-2059.
218. Tatarchuk, T., Bououdina, M., Paliychuk, N., Yaremiy, I., Moklyak, V. (2017). Structural characterization and antistructure modeling of cobalt-substituted zinc ferrites. *Journal of Alloys and Compounds*; 694:777-791.
219. Manjari, G. (2018). Green synthesis of silver and copper nanoparticles using Aglaia elaeagnoidea and its catalytic application on dye degradation, in, Department of Ecology and Environmental Sciences, Pondicherry University,
220. Sundararajan, M., Sailaja, V., Kennedy, L.J., Vijaya, J.J. (2017). Photocatalytic degradation of rhodamine B under visible light using nanostructured zinc doped cobalt ferrite: kinetics and mechanism. *Ceramics International*; 43:540-548.
221. Singh, S., Srinivas, C., Tirupanyam, B., Prajapat, C., Singh, M., Meena, S., et al. (2016). Structural, thermal and magnetic studies of MgxZn1− xFe2O4 nanoferrites: study of exchange interactions on magnetic anisotropy. *Ceramics International*; 42:19179-19186.
222. Manikandan, A., Kennedy, L.J., Bououdina, M., Vijaya, J.J. (2014). Synthesis, optical and magnetic properties of pure and Co-doped ZnFe2O4 nanoparticles by microwave combustion method. *Journal of Magnetism and Magnetic Materials*; 349:249- 258.
223. Manikandan, A., Vijaya, J.J., Kennedy, L.J., Bououdina, M. (2013). Structural, optical and magnetic properties of

Zn1− xCuxFe2O4 nanoparticles prepared by microwave combustion method. *Journal of Molecular Structure*; 1035:332-340.

224. Angadi, V.J., Anupama, A., Choudhary, H.K., Kumar, R., Somashekarappa, H., et al. (2017). Mechanism of γ-irradiation induced phase transformations in nanocrystalline Mn0. 5Zn0. 5Fe2O4 ceramics. *Journal of Solid-State Chemistry*; 246:119-124.
225. Jesudoss, S., Vijaya, J.J., Kennedy, L.J., Rajan, P.I., Al-Lohedan, H.A., et al. (2016). Studies on the efficient dual performance of Mn1–xNixFe2O4 spinel nanoparticles in photodegradation and antibacterial activity. Journal of Photochemistry and Photobiology B: Biology; 165:121-132.
226. Kumar, R., Kar, M. (2016). Correlation between lattice strain and magnetic behavior in nonmagnetic Ca substituted nano-crystalline cobalt ferrite. *Ceramics International*; 42:6640-6647.
227. Sonia, M.M.L., Anand, S., Vinosel, V.M., Janifer, M.A., Pauline, S., et al. (2018). Effect of lattice strain on structure, morphology and magneto-dielectric properties of spinel NiGdxFe2− xO4 ferrite nano-crystallites synthesized by sol-gel route. *Journal of Magnetism and Magnetic Materials*; 466:238-251.
228. Sonia, M.M.L., Anand, S., Vinosel, V.M., Janifer, M.A., Pauline, S. (2018). Effect of lattice strain on structural, magnetic and dielectric properties of sol–gel synthesized nanocrystalline Ce 3+ substituted nickel ferrite. Journal of Materials Science: *Materials in Electronics*; 29:15006-15021.
229. Gul, S., Yousuf, M.A., Anwar, A., Warsi, M.F., Agboola, P.O., et al. (2020). Al-substituted zinc spinel ferrite nanoparticles: Preparation and evaluation of structural, electrical, magnetic and photocatalytic properties. *Ceramics International*; 46:14195-14205.
230. Muthuselvam, I.P., Bhowmik, R. (2010). Mechanical alloyed Ho3+ doping in CoFe2O4 spinel ferrite and understanding of magnetic nanodomains. *Journal of Magnetism and Magnetic Materials*; 322:767-776.
231. Yadav, R.S., Havlica, J., Hnatko, M., Šajgalík, P., Alexander, C., et al. (2015). Magnetic properties of Co1− xZnxFe2O4 spinel ferrite nanoparticles synthesized by starch-assisted sol–gel autocombustion method and its ball milling. *Journal of Magnetism and Magnetic Materials*; 378:190-199.
232. Srinivas, Ch., Tirupanyam, B.V., Meena, S.S., Yusuf, S.M., Seshu Babu, Ch., et al. (2016). Structural and magnetic characterization of co-precipitated NixZn1−xFe2O4 ferrite nanoparticles. *Journal of Magnetism and Magnetic Materials*; 407:135-141.
233. Prasad, S., Deepty, M., Ramesh, P., Prasad, G., Srinivasarao, K., et al. (2018). Synthesis of MFe2O4 (M= Mg2+, Zn2+, Mn2+) spinel ferrites and their structural, elastic and electron magnetic resonance properties. *Ceramics International*; 44:10517-10524.
234. Gabal, M., El-Shishtawy, R.M., Al Angari, Y. (2012). Structural and magnetic properties of nano-crystalline Ni–Zn ferrites synthesized using egg-white precursor. *Journal of Magnetism and Magnetic Materials*; 324:2258-2264.
235. Jacob, B.P., Thankachan, S., Xavier, S., Mohammed, E. (2011). Effect of Gd3+ doping on the structural and magnetic properties of nanocrystalline Ni–Cd mixed ferrite. *Physica Scripta*; 84:045702.
236. Junaid, M., Khan, M.A., Akhtar, M.N., Hussain, A., Warsi, M.F. (2019). Impact of indium substitution on dielectric and magnetic properties of Cu0. 5Ni0. 5Fe2-xO4 ferrite materials. *Ceramics International*; 45:13431-13437.
237. Thakur, A., Thakur, P., Hsu, J.-H. (2014). Structural, Magnetic and Electromagnetic Characterization of In3+ Substituted Mn-Zn Nanoferrites, *Zeitschrift für Physikalische Chemie*; 228:663-672.
238. Anwar, H., Maqsood, A. (2012). Effect of sintering temperature on structural, electrical and dielectric parameters of Mn-Zn nano ferrites, in: Key Engineering Materials. *Trans Tech Publ*: 163-170.
239. Pereira, C., Pereira, A.M., Fernandes, C., Rocha, M., Mendes, R., et al. (2012). Superparamagnetic MFe2O4 (M= Fe, Co, Mn) nanoparticles: tuning the particle size and magnetic properties through a novel one-step coprecipitation route. *Chemistry of Materials*; 24:1496-1504.
240. Ni, H., Gao, Z., Li, X., Xiao, Y., Wang, Y., et al. (2018). Synthesis and characterization of CuFeMnO4 prepared by co-precipitation method. *Journal of Materials Science*; 53:3581-3589.
241. Velmurugan, K., Venkatachalapathy, V.S.K., Sendhilnathan, S. (2010). Synthesis of nickel zinc iron nanoparticles by coprecipitation technique. *Materials Research*; 13:299-303.
242. Hoshi, K., Kato, H., Fukunaga, T., Furusawa, S., Sakurai, H. (2013). Synthesis of MnZn ferrite using coprecipitation method, in: key engineering materials, *Trans Tech Publ*: 22-25.
243. Houshiar, M., Zebhi, F., Razi, Z.J., Alidoust, A., Askari, Z. (2014). Synthesis of cobalt ferrite (CoFe2O4) nanoparticles using combustion, coprecipitation, and precipitation methods: A comparison study of size, structural, and magnetic properties. *Journal of Magnetism and Magnetic Materials*; 371:43-48.
244. Kaur, N., Kaur, M. (2014). Comparative studies on impact of synthesis methods on structural and magnetic properties of magnesium ferrite nanoparticles. *Processing and Application of Ceramics*; 8:137-143.
245. Lungu, A., Malaescu, I., Marin, C., Vlazan, P., Sfirloaga, P. (2015). The electrical properties of manganese ferrite powders prepared by two different methods. *Physica B: Condensed Matter*; 462:80-85.
246. Issa, B., Obaidat, I., Albiss, B., Haik, Y. (2013). Magnetic nanoparticles: surface effects and properties related to biomedicine applications. *Int. J. Mol. Sci*; 14:21266–21305.
247. Singamaneni, S., Bliznyuk, V.N., Binek, C., Tsymbal, E.Y. (2011). Magnetic nanoparticles: recent advances in synthesis, self-assembly and applications. *J. Mater. Chem*; 21:16819–16845.